FACIES ANALYSIS AND DEPOSITIONAL SEQUENCES OF THE UPPER JURASSIC MOZDURAN FORMATION, A CARBONATE RESERVOIR IN THE KOPET DAGH BASIN, NE IRAN

M. A. Kavoosi*+, Y. Lasemi**, S. Sherkati* and R. Moussavi-Harami***

Upper Jurassic carbonates of the Mozduran Formation constitute the principal reservoir intervals at the giant Khangiran and Gonbadli gasfields in the Kopet Dagh Basin, NE Iran. These carbonates were investigated using detailed field studies and petrographic and wireline log analyses in order to clarify their depositional facies and sequence stratigraphy. Facies were interpreted to reflect deep basin, fore-shoal, shelf margin, lagoon, tidal flat and coastal plain depositional systems.

The Mozduran Formation is composed of six depositional sequences. Thickness variations were controlled by differential subsidence. Aggradation on the platform margin and reduced carbonate production in the deep basin together with differential subsidence resulted in the creation of a narrow seaway during the late Oxfordian. Petrographic studies suggest that Mozduran Formation carbonates had a low-Mg calcite mineralogy during the Oxfordian, and an aragonite to high-Mg calcite mineralogy during the Kimmeridgian. Reservoir pay zones are located in highstand systems tracts within the lower and middle Kimmeridgian depositional sequences. The rapid lateral thickness variations of these sequences were controlled by tectonic factors, leading to compartmentalization of the Mozduran Formation reservoir with the possible creation of stratigraphic traps, especially at the Khangiran field.

INTRODUCTION

The Kopet Dagh orogenic belt is an inverted basin (Allen *et al*., 2003) extending from the east of the Caspian Sea to NE Iran, Turkmenistan and north Afghanistan (Afshar-Harb, 1979; Buryakovsky *et al*., 2001). The belt separates the Turan Shield from central Iran (Jackson *et al*., 2002). Following the closure of Palaeo-Tethys in the Middle Triassic (Alavi *et al*., 1997) and the opening of Neo-Tethys during the Early to Middle Jurassic (Buryakovsky *et al*., 2001), the Kopet Dagh Basin formed in an extensional regime during the Early to Middle Jurassic (Garzanti and Gaetani, 2002). Over 6000 m of sedimentary rocks ranging in age from Middle Jurassic to Miocene were deposited in the basin (Afshar-Harb, 1979) and can be assigned to five major transgressive-regressive sequences (Moussavi-Harami and Brenner, 1992). Jurassic-Cenozoic carbonates and siliciclastics unconformably overlie Palaeozoic (basement) and Triassic rocks (Ulmishek, 2004).

The Kopet Dagh Basin hosts the giant *Khangiran* and *Gonbadli* gasfields (Fig. 1) discovered in 1968 and 1969 respectively, which produce mainly from the Upper Jurassic Mozduran Formation. This formation is composed principally of limestones and dolomites with minor marl/shales, sandstones and evaporites, and crops out along the Kopet Dagh Range. Lower Cretaceous siliciclastics of the Shurijeh Formation (Fig. 2) form an additional reservoir. The

* National Iran Oil Company Exploration Directorate, 1st Deadend, Seoul Street, NE Sheikh Bahaei Square, PO Box 19395-6669, Tehran, Iran.
** Department of Geology, Teachers Training University, No.49, Mofateh Ave, Tehran 15614, Iran.
*** Department of Geology, Ferdowsi University, Mashhad, Iran.
+ Corresponding author. m.kavoosi@niocexp.ir

Key words: Kopet Dagh Basin, Upper Jurassic, Mozduran Formation, facies analysis, sequence stratigraphy, reservoir, Iran, carbonates.

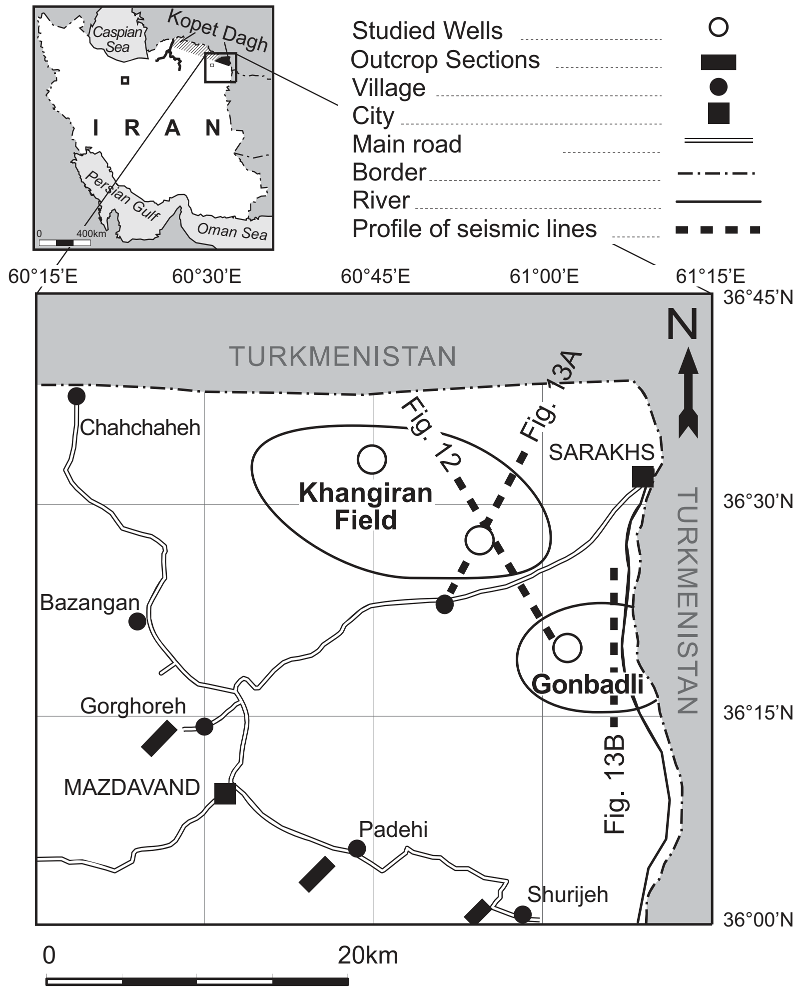

Fig. 1. Location map of the study area in NE Iran. Localities include the *Khangiran* and *Gonbadli* gasfields, and the outcrop locations at Ghorghoreh, Padehi and Shurijeh at which stratigraphic sections were measured.

structures at *Khangiran* and *Gonbadli* were formed during Tertiary shortening (Ulmishek, 2004). The major source rock interval occurs in the Middle–Upper Jurassic shales and carbonates of the Chaman Bid Formation (Fig. 2) (Afshar-Harb, 1979; Mahboubi *et al*., 2001); upper Bajocian to Bathonian mudstones of the Kashafrud Formation may also have generated hydrocarbons (Poursoltani *et al*., 2007).

The objective of this study is to report on facies variations, depositional environments and sequence stratigraphy of Upper Jurassic sediments in the Mozduran Formation in the east of the Kopet Dagh Basin. Previous studies of the formation (Adabi and Rao, 1991; Lasemi, 1995) focussed on outcrops in the Kopet Dagh Mountains and did not discuss the formation's reservoir properties at *Khangiran* and *Gonbadli*.

GEOLOGIC AND STRATIGRAPHIC SETTING

Basement in the Kopet Dagh Basin is exposed at Aghdarband in the south and is composed of sedimentary and igneous rocks (Devonian to Triassic), which were intensely deformed during the Hercynian and Cimmerian orogenies (Shahriari *et al*., 2005). Following the closure of Palaeo-Tethys during the Middle to Late Triassic (e.g. Alavi, 1991), the Kopet Dagh Basin underwent thermal subsidence, which reached a maximum in the Jurassic (Poursoltani *et al*., 2007). Sedimentation on the southern Turan Platform began in the Middle Jurassic (Lyberis and Manby, 1999) with a sedimentary package which thickens from southern Turkmenistan to NE Iran. Zones of abrupt thickening are indicative of extensional faults (Thomas *et al*., 1999a; Lyberis and Manby, 1999). The basin was the site of relatively continuous sedimentation from the Jurassic to the Miocene (Afshar-Harb, 1979, 1982).

During the Kimmeridgian–Tithonian, the Turan Platform underwent regional uplift due to the collision of the south-central Afghanistan (Helmand) and Qatang microcontinents with the southern margin of Eurasia (Golonka, 2004). Seyed-Emami *et al*. (2004) suggested that the late Cimmerian tectonic phase resulted in widespread Late Jurassic – Early

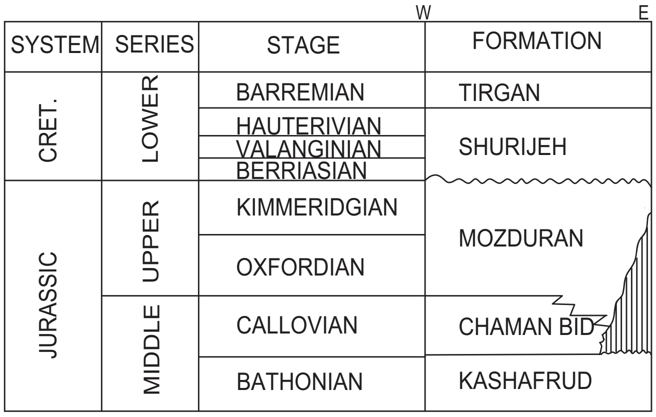

Fig. 2. Stratigraphic nomenclature for the Jurassic and Lower Cretaceous in the eastern Kopet Dagh Basin.

Cretaceous regression, leading to deposition of the Lower Cretaceous continental siliciclastics of the Shurijeh Formation (Fig. 2). Widespread Jurassic – Miocene marine carbonates and siliciclastics were deformed into a series of folds and thrusts (Allen *et al*., 2003) as a result of collision between the Lut Plate and the Turan Platform during the Oligocene – middle Miocene (Kopp, 1997). This collision led to crustal shortening and right-lateral transpression (Brunet *et al*., 2003) which is still continuing as indicated by seismic activity (Thomas *et al*., 1999; Golonka, 2004). Patterns of deformation generally follow the pre-Jurassic structural grain (Ulmishek, 2004).

During the Callovian, a marine transgression from the NW resulted in the deposition of Upper Jurassic carbonates of the Mozduran Formation above the Bajocian–Bathonian siliciclastic deposits of the Kashafrud Formation (Lasemi, 1995). The contact between the Mozduran and Kashafrud Formations in the eastern Kopet Dagh is unconformable; to the west, the contact is conformable and gradational with deeper-marine Bathonian to Oxfordian carbonates and shales/marls of the Chaman Bid Formation (Fig. 2). To the east of the Kopet Dagh Range, the Chaman Bid Formation disappears and the base of the Mozduran Formation is Oxfordian (Afshar-Harb, 1979; Aghanabati, 2004), which implies a Callovian hiatus. The Mozduran Formation becomes younger from west to east and from the *Khangiran* and *Gonbadli* structures southwards towards the outcrop locations (Fig. 1). This trend is accompanied by an eastward transition of the Mozduran Formation to evaporites and siliciclastic sediments with an obvious decrease in thickness in the eastern part of the Iranian Kopet Dagh Range.

The Mozduran Formation is disconformably overlain by Lower Cretaceous siliciclastics of the Shurijeh Formation (Fig. 2). The biostratigraphic and chronostratigraphic framework is well established based on foraminifera as well as calpionelids (Kalantari, 1969, 1986; Afshar-Harb, 1969, 1979, 1982).

MATERIALS AND METHODS

Detailed field studies, microscope-based investigations, microfacies and wireline log analyses were carried out on three outcrop sections (Ghorghoreh, Padehi and Shurijeh) and on well successions at the *Khangiran* and *Gonbadli* gasfields (Fig. 1). Over 2000 samples of the Upper Jurassic Mozduran Formation from the gasfields and the outcrops were studied. Thin sections from outcrop sections, well cuttings and cores together with well logs (gamma ray, sonic, density, neutron and resistivity) were used, as well as seismic images from the east of the study area (profile locations in Fig. 1).

Surface sections were measured using a Jacob Staff and directional samples were taken systematically every two metres during logging. Samples were collected where significant facies and lithological changes were observed to enhance field studies. Thin sections were studied for petrographic and facies analyses. The thin sections were stained with Alizarin-Red S (Dickson, 1965) to detect dolomitization of grains especially cements. The grains and matrix percentages were estimated using visual percentage charts (Flügel, 1982). Dunham's classification (1962) was used for carbonate facies nomenclature with the exception that the upper size-limit for micrite was set at 0.06 mm. Diagenetic features were studied using a catholuminescence microscope (*Nikon CL, CCL 8200*) at the Research Institute of Petroleum Industry of the National Iranian Oil Company. Sandstones were classified using the Pettijohn *et al*. (1987) system. Facies types and depositional settings were interpreted based on compositional, textural, fabric and sedimentary data and by comparison with modern environments (e.g. Purser, 1973; Wilson, 1975; Tucker and Wright, 1990; Flügel, 2004).

Palaeoenvironmental reconstruction and sequence stratigraphic interpretation is based on outcrop observations, core and wireline logs, and seismic profiles. Sedimentary structures, stratal stacking patterns, geometry and the sequence boundaries of

	E	D	C	B	A
Facies/Facies association	E1: Lime mudstone E2: Dolomudstone E3: Gypsum/Anhydrite E4: Stromatolite boundstone E5: Peloid grainstone	D1: Ostracod wackestone D2: Bioclastic wackestone/packstone D3: Bioclastic peloid packstone D4: Oncoid packstone	C1: Ooid grainstone C2: Bioclastic peloid ooid grainstone C3: Bioclastic packstone	B1: Tubiphytes packstone/boundstone B2: Brachiopod packstone B3: Thrombolite boundstone B4: Microbialite boundstone	A1: Lime mudstone A2: Radiolarian wackestone A3: Sponge spicule wackestone A4: Bioclastic packstone
Sedimentary Structures/ Fabric	erosional surfaces, graded bedding, lamination, solution breccia, geopetal fabrics, fenestral fabric	Lamination, erosional surfaces, fenestral fabric, bioturbation	Lamination, cross-bedding, geopetal, cross-lamination, erosional surfaces	geopetal fabric, vadose silt, cross-bedding, lamination	bioturbation, erosional surfaces, lamination, graded bedding
Main Components	peloids, ostracod, microbolites, gastropods, intraclasts, silt, sand	ooid, peloid, microbolites, gastropod, Cayauxia, dasyclads, Clypeina, sand, Pesudocyclammina, Salpingoporella, Lithocodium, miliolid, benthic forams, echinoid, Codicea, molluscs, shells	peloids, gastropods, brachiopods, Cayauxia, dasyclads, Tubiphytes Lithocodium, benthic forams, sand echinoid, algae, corals, pelecypods	peloids, gastropods, brachiopods, Tubiphytes, stomatoporoid, serpulid, Lithocodium, echinoid, coral, pelecypod, sponge spicules, microbolites, planktonic bivalves/filaments	peloid, ooid, intraclast, gastropod, brachiopods, Tubiphytes, stomatoporoid, serpulid, echinoids, coral, pelecypod,sponge spicule, microbolites, planktonic bivalves, red algae, ostracod, bryozoa, minor benthic forams, belemnites, tintinnids, calpionelids, radiolarids
Depositional Environments	Supratidal/Sabkha, Intertidal	Shelf-Lagoon	Shelf-margin	Fore-shoal	Basin

Table 1. Facies / facies association, sedimentary structures, main components and depositional settings of the Mozduran Formation carbonates in the study area.

the carbonate and siliciclastic rocks were considered during field studies.

CARBONATE FACIES

Field, petrographic, core and wireline log analyses of the Mozduran Formation in the study area led to the recognition of basinal, fore-shoal, shelf margin, restricted to semi-restricted shelf lagoon and tidal flat/ beach facies belts which were deposited on a narrow rimmed carbonate shelf. Siliciclastic facies were deposited in an adjacent nearshore setting. The facies are considered briefly in turn below.

Basinal facies

This facies comprised lime mudstones, radiolarian wackestones, sponge spicule wackestones and bioclastic packstones (Table 1). Bioclasts included radiolarids, calpionelids, planktonic foraminifera, sponge spicules, echinoid/crinoid fragments and filaments. Features present within this facies include bioturbation and erosional surfaces. Pyrite is abundant in upper Oxfordian carbonates at well *Khangiran-30*. The basinal facies belt was only observed at the *Khangiran* and *Gonbadli* gasfields; their thickness increased from *Gonbadli* towards *Khangiran* (Fig. 1).

Interpretation

The dominance of planktonic foraminifera, radiolarids, calpionelids and sponge spicules, the scarcity of benthic foraminifera and the lack of sedimentary structures accompanied by pyritization suggest a deep-water dysoxic depositional environment below storm wave base.

Fore-shoal facies

Fore-shoal sediments include tubiphyte packstone/ boundstones, brachiopod packstones, thrombolite boundstones and microbialite boundstones (Table 1), which separate open-marine from shelf-margin facies. The fore-shoal facies belt has the greatest distribution at the *Khangiran* and *Gonbadli* gasfields. Its thickness decreased from *Khangiran* towards *Gonbadli* during the Oxfordian (Fig. 1), but decreased from *Gonbadli* to *Khangiran* during the Kimmeridgian.

Interpretation

Microbialites result mainly from the activity of cyano- and other bacteria, but micro-encrusters such as foraminifera and small metazoans may also contribute (Chafetz, 1986; Riding, 1991, 2006). In general, water energy and sedimentation rate control the macroscopic and mesoscopic growth-form of microbialites (e.g. Keupp *et al*., 1993). Low-relief growth types develop under conditions of moderate to high sedimentation rate (Olivier *et al*., 2003). Tubiphytes and thrombolites occur up to the base of the fore-slope (Seeling *et al*., 2005). Rising sea-levels favour microbialite development (Cabioch *et al*., 2006). Changes from nodular to thick, massive bedding indicate a shallower depositional environment than for carbonate nodules (Carpentier *et al*., 2007).

Shelf-margin facies

Shelf-margin sediments are characterized by ooid grainstones, bioclast peloid and ooid grainstones, and bioclastic packstones (Table 1) which separate the fore-shoal and restricted lagoon facies. Shelf-margin facies occur in thick to massive units with lamination, cross-bedding and erosional surfaces. Some ooids show diagenetic modification such as dolomitization and dissolution in Kimmeridgian carbonates at *Khangiran* and *Gonbadli* (e.g. well *Khangiran 30)*. Cross-bedding with reactivation surfaces, large- to medium-scale parallel lamination, planar cross-bedding and trough cross-bedding were observed. Ooids with quartz and bioclastic nuclei had radial and concentric cortices at outcrops of the study area in the Oxfordian and upper Kimmeridgian deposits.

Interpretation

The presence of lamination, cross-bedding and erosional surfaces indicates wave and current activity in a high-energy depositional environment, supported by the presence of grain-supported and mud-free textures (Lucia, 1999; Palma *et al*., 2007). Development of micritic envelopes indicates low sedimentation rates (Palma *et al*., 2007) within the photic zone. On the Bahamas Platform, ooids are generated in carbonate shoals in water depth of 2-5 m (Flügel, 1982, 2004; Tucker and Wright, 1990). A relationship between dry climate, hypersalinity and ooid formation was suggested by Selley (1999) and Husinec and Read (2007).

Lagoonal facies

Lagoonal facies are characterized by ostracod wackestones, bioclastic wackestone/packstones, bioclastic peloid packstones and oncoid packstones (Table 1). Ostracod wackestones contain calcite pseudomorphs after anhydrite/gypsum with no evidence of subaerial exposure. The facies is cream to brown in colour and thin- to medium-bedded.

Interpretation

The presence of ostracod fragments indicates the restricted circulation of open-marine waters across the platform (El-Tabakh *et al*., 2004). Dasycladacean algae and *Cayeuxia* are common in lagoonal environments (Palma *et al*., 2007). Highly bioturbated carbonates indicate a shallow-marine environment, suggesting a low sedimentation rate (Strasser *et al*., 1999). Bioclastic peloid packstones suggest higher-energy conditions in a shallow subtidal setting (e.g. Lasemi, 1995). The wackestone and packstone textures indicate deposition in the proximal part of a subtidal lagoon (Lasemi *et al*., 2008). Oncoids are in general formed during low sedimentation rates and periodic weak water agitation (Gradzinski *et al*., 2004). Oncoids are common in the upper part of lagoonal successions (Seeling *et al*., 2005). Lagoonal facies have the greatest thickness at the Ghorghoreh outcrop section.

Tidal flat facies

Tidal flat facies are in general composed of lime mudstones, dolomudstones, gypsum/anhydrite nodules/layers, flat laminated to wavy stromatolite boundstones and peloid grainstones (Table 1). Lime mudstones display mm-thick, straight to wavy lamination with fenestral/birds-eye fabrics and sparse microbial filaments. Laminated lime mudstones were observed below and on top of stromatolite boundstones and dolomudstones. Dolomudstone with calcite pseudomorphs after gypsum/anhydrite was observed in thin-bedded, cream coloured intervals interbedded with evaporite nodules/layers. Tidal flat facies have the widest distribution in the upper Kimmeridgian deposits in the study area especially at the *Khangiran* and *Gonbadli* structures. Collapse breccias were observed at Padehi, Ghorghoreh and the Mozduran Formation type section. Peloid grainstones with a keystone fabric were composed mainly of peloid grains of various origins.

Interpretation

Sedimentary structures and fabrics (erosional surfaces, graded bedding, lamination, solution breccias, mud cracks and fenestral fabrics together with calcite pseudomorphs after gypsum/anhydrite and red-beds) suggest deposition in a low-energy supratidal environment. Dolomudstone with birds-eyes and discontinuous laminae with calcite pseudomorphs after gypsum/anhydrite are interpreted to indicate deposition in an upper intertidal to supratidal environment (e.g. Shinn, 1983a, b).

Sedimentary structures such as erosional surfaces, gutters-and-pots, graded bedding with sharp basal and gradational upper contacts (Figs 3A-3D) are evidence of tempestites (e.g. Aigner, 1982, 1985). Graded bedding, sharp basal contacts and poor sorting in peloid grainstone and intraclast grainstone/packstones are interpreted as storm-influenced deposits (Aigner, 1985; Flügel, 1982, 2004). This interpretation is supported by the discontinuous facies relationships that are expressed at locations where the intraclast

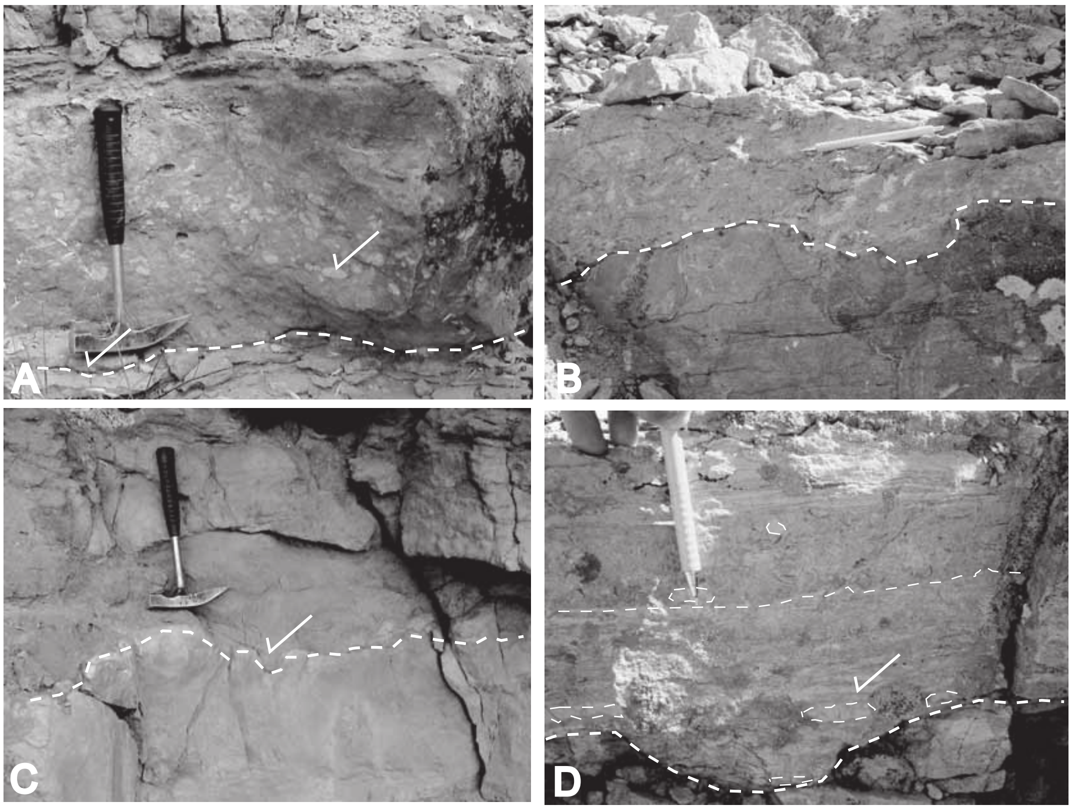

Fig. 3. Field photographs of tempestite/storm facies. (A) Intraclast wackestone/packstone with basal erosional contact. (B) Bioclastic intraclast packstone, with an erosional lower surface. (C) Gutter cast below storm deposit. (D) Intraclast packstone with basal erosional surface which passes into laminated bioclastic packstone/wackestone.

packstones are intercalated with mudstones. The keystone peloid grainstone/packstone textures and its vertical association with lagoonal and upper intertidal/ supratidal facies indicate deposition in a lower intertidal sub-environment (Lasemi *et al*., 2008). The low diversity faunal assemblage implies stressed palaeo-ecological conditions such as elevated salinities.

At the present day, stromatolites form in the lower intertidal zone in the Persian Gulf (Purser, 1973; Shinn, 1983a, b). Although laminated stromatolites develop in upper intertidal to lower supratidal settings (Palma *et al*., 2007), the presence of calcite pseudomorphs after gypsum/anhydrite in stromatolite boundstones in the Mozduran Formation indicates deposition in an arid, lower intertidal setting.

In summary, these characteristics of the Mozduran Formation indicate deposition on arid tidal flats, similar to those of carbonate tidal flats of the present-day Persian Gulf (Purser, 1973; Chafetz *et al*., 19994).

Siliciclastic facies

Siliciclastic sediments of the Mozduran Formation comprise sand to clay-grade material. Ripple marks (bifurcated, wavy and current), cross bedding (planar and trough), and lamination are the main sedimentary structures in the sandstone layers. Sandstones comprise quartzarenites, feldspathic litharenites, chertarenites and lithic greywackes. Siliciclastics have their greatest areal distribution in the easternmost part of the Kopet Dagh Range including the Shurijeh surface section (Figs. 1, 7), and their smallest distribution in the area around the *Khangiran* field.

Interpretation

The presence of bifurcated ripple marks indicates the dominance of waves over currents during sedimentation (c.f Reineck and Singh, 1980). The wave-rippled sandstones at the base of the succession are indicative of a beach environment. Current ripple-marks that overlie bifurcated ripple marks indicate the influence of tidal currents. The low frequency or absence of bioturbation in the fining-upward sandstones indicates high tidal current velocities and high suspended loads (Leeder, 1999). Coarsening- and thickening-upward feldspathic litharenites indicate beach settings. Low-angle stratification, the well sorted nature of the sandstones together with rounded grain outlines also indicate a beach-type depositional setting (c.f. Nichols, 2000), as do wave ripples and horizontal lamination (El-Azabi and El-Araby, 2007). Red siltstones and mudstones and thin fining-upward cycles can be interpreted in terms of of flood plain deposition.

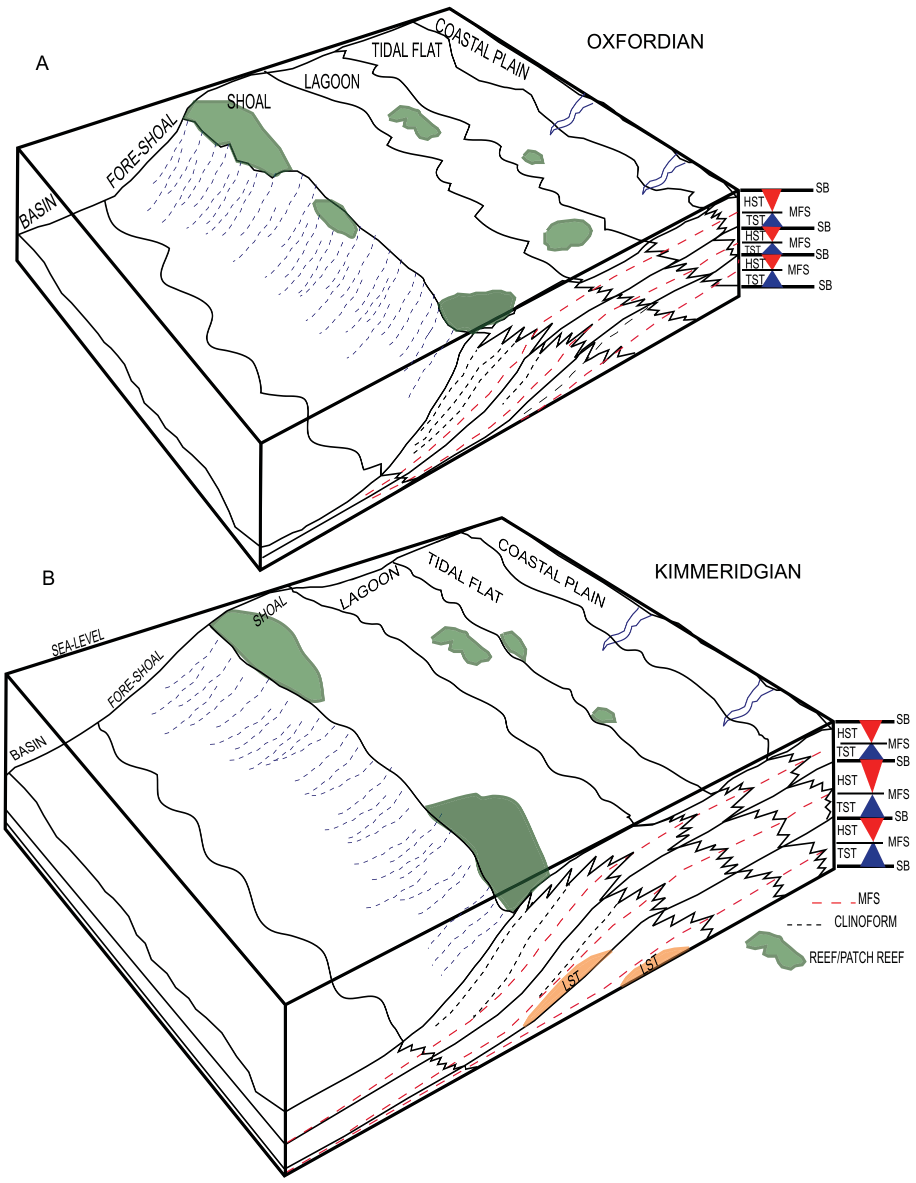

Fig. 4. Depositional model for Upper Jurassic deposits in the study area. (A) Depositional model for the platform carbonates of the Mozduran Formation and its deep-marine equivalent (the Chaman Bid Formation) during the Oxfordian, with depositional sequences. (B) Depositional model for the Mozduran Formation showing progradation of depositional sequences and development of a carbonate platform during the Kimmeridgian. Note the evolution from a rimmed shelf to a ramp during the late Kimmeridgian.

DEPOSITIONAL MODEL

The studied sections and wells indicate that there was a sharp transition from a siliciclastic-dominated shallow-marine coastal plain in the east to a deep basin in the north and west. Deposition on a rimmed carbonate platform (c.f. Read, 1982, 1985; Tucker and Wright, 1990) is inferred, passing into a carbonate ramp during the late Kimmeridgian (Kavoosi *et al*., 2008). Our studies indicate that the carbonates of the Mozduran Formation (carbonate platform) pass into the Chaman Bid Formation (deeper-marine basin) to the west, and into paralic deposits to the east (Figs 4A, 4B). The basinal environment was characterized by pelagic facies containing ammonites, radiolarids, belemnites, sponge spicules and fine-to coarse-grained calciturbidites shed from the Mozduran Formation platform margin.

Two depositional models can therefore be defined for the Upper Jurassic sediments of the Mozduran Formation. During the Oxfordian, a microbial dominated platform developed with a nearby deep-marine basin (Fig. 4A). The creation of seaways was associated with microbial facies development and sea-level rise during the late Oxfordian. By contrast during the late Kimmeridgian, there was a transition from a rimmed shelf to a carbonate ramp (Fig. 4B). During the late Kimmeridgian, an oolite- dominated ramp developed in the Kopet Dagh Basin. The transition from a rimmed shelf to a carbonate ramp during Mozduran Formation sedimentation was accompanied by a climatic change. This is indicated by toplap terminations of seismic reflections (see Fig. 12 below) indicating non-deposition. The presence of "hummocky" geometry above the toplap surface suggests deposition by turbidity currents in a submarine fan. The presence of siliciclastic deposits with plant remains, especially at the Padehi surface section, is consistent with this interpretation.

Seaways that developed during the late Oxfordian were filled with calciturbidites, siliciclastics and evaporites during the Kimmeridgian. The Mozduran Formation includes evidence of deposition on a storm-dominated ramp during the late Kimmeridgian (Fig. 4B). Deposition took place under arid climatic conditions during the Kimmeridgian and a temperate climate in the late Kimmeridgian. Arid conditions are indicated by the presence of evaporites, calcite pseudomorphs and red-beds (siltstone/claystone and lime mudstones).

DEPOSITIONAL SEQUENCES

The sequence stratigraphic model applied here follows Van Wagoner *et al*. (1988, 1990). Both sequence boundaries and transgressive surface were used to identify depositional sequences at outcrop and in the subsurface. Third-order depositional sequences correspond to long-term changes of relative sea-level (Vail *et al*., 1991), and lower order sequences are attributed to sea-level fluctuations in the Milankovitch frequency band (Pittet *et al*., 2000).

Gamma-ray logs can be used for general facies interpretations (Pawellek and Aigner, 2003). Facies analyses, parasequence stacking patterns and shifts in the gamma-ray, density, neutron, sonic and resistivity logs were used to identify LSTs, TSTs and HSTs. The Upper Jurassic Mozduran Formation in the Kopet Dagh Basin consists primarily of asymmetric, high frequency (fourth- to six-order) shallowing-upward parasequences (c.f. van Wagoner *et al*., 1988). Six depositional sequences are recognised and are described briefly in turn below:

1. Depositional Sequence 1: Oxfordian (OX1)

TST deposits of sequence OX1 (lower Oxfordian) at the Ghorghoreh outcrop section (Fig. 5) are characterized by an aggradational parasequence stacking pattern. The MFS is accompanied by massive dolomitized bioclastic grainstones which contain an open-marine fauna. At the Padehi section (Fig. 6), the TST is thin and is composed mainly of lagoonal facies. From this location towards the *Khangiran* and *Gonbadli* gasfields (Fig. 1), the TST is characterized by fore-shoal and deep-basin facies (Figs 8, 9).

The MFS on the platform is indicated by a maximum rate of carbonate production and aggradation (Handford and Loucks, 1993). At *Khangiran* and *Gonbadli,* the MFS was recognized by the presence of radiolarids, calpionellids, *Saccocoma* and planktonic foraminifera (Figs 8, 9), indicating a deep-marine pelagic to hemipelagic depositional setting (McIlreath and James, 1984).

HST deposits of sequence OX1 at the Ghorghoreh section (Fig. 5) are characterized by three shallowing- and thinning-upward parasequence sets together with more restricted facies, which suggest a progradational stacking pattern. Thinning-upwards trends commonly occur in highstand systems tracts in fully aggraded flat-top platforms (e.g. Montañez and Osleger, 1993). This is consistent with the shallowing-upward trend of facies at *Khangiran-30* and *Gonbadli-2* (Figs. 8, 9). At the *Khangiran* and *Gonbadli* gasfields, in addition to vertical facies changes, the HST was recognized by a gradual decrease in gamma-ray log reading due to high carbonate production as the result of decreasing of micrite and increasing grain size. The late HST was characterized by the progradation of tidal flat facies containing lime mudstones with evaporite casts/pseudomorphs, on lagoonal and shelf-margin facies respectively. Bioclastic wackestones, *Tubiphytes* packstones and peloid packstone/grainstones are in turn overlain by lime mudstones containing evaporite casts/pesudomorphs.

Sequence OX1 was not deposited at the Shurijeh location (Fig. 7). The lack of accommodation in the Shurijeh area is a result of the presence of a palaeohigh as indicated by the presence of exposed basement rocks, the thin sedimentary package and stratigraphic gaps.

The lower sequence boundary of the OX1 sequence is type 1 at outcrop locations and *Gonbadli* and type 2 at *Khangiran-30* (Fig. 9). The upper sequence boundary is type 1 in the study area.

2. Depositional Sequence 2: Oxfordian (OX2)

At the *Khangiran* and *Gonbadli* gasfields and at the Shurijeh, Padehi and Ghorghoreh outcrop locations (Fig. 1), LST deposits include lithic greywackes, siltstones and claystones.

The transgressive systems tract in sequence OX2 include a wide range of depositional facies from shore-face to fore-shoal. TST deposits are characterized by stromatolite boundstones and thrombolite patch reefs (Figs 5, 6, 7, 8, 9). Thrombolites are characteristic of reduced sedimentation rates and sea-level rise (Leinfelder, 1993; Parcell, 2001; Whalen *et al*., 2002; Lasemi and Amin-Rassouli, 2007). The vertical amalgamation of inlet channels and shelf-margin facies indicate an aggradational stacking pattern within the TST. During aggradation, coated-grain

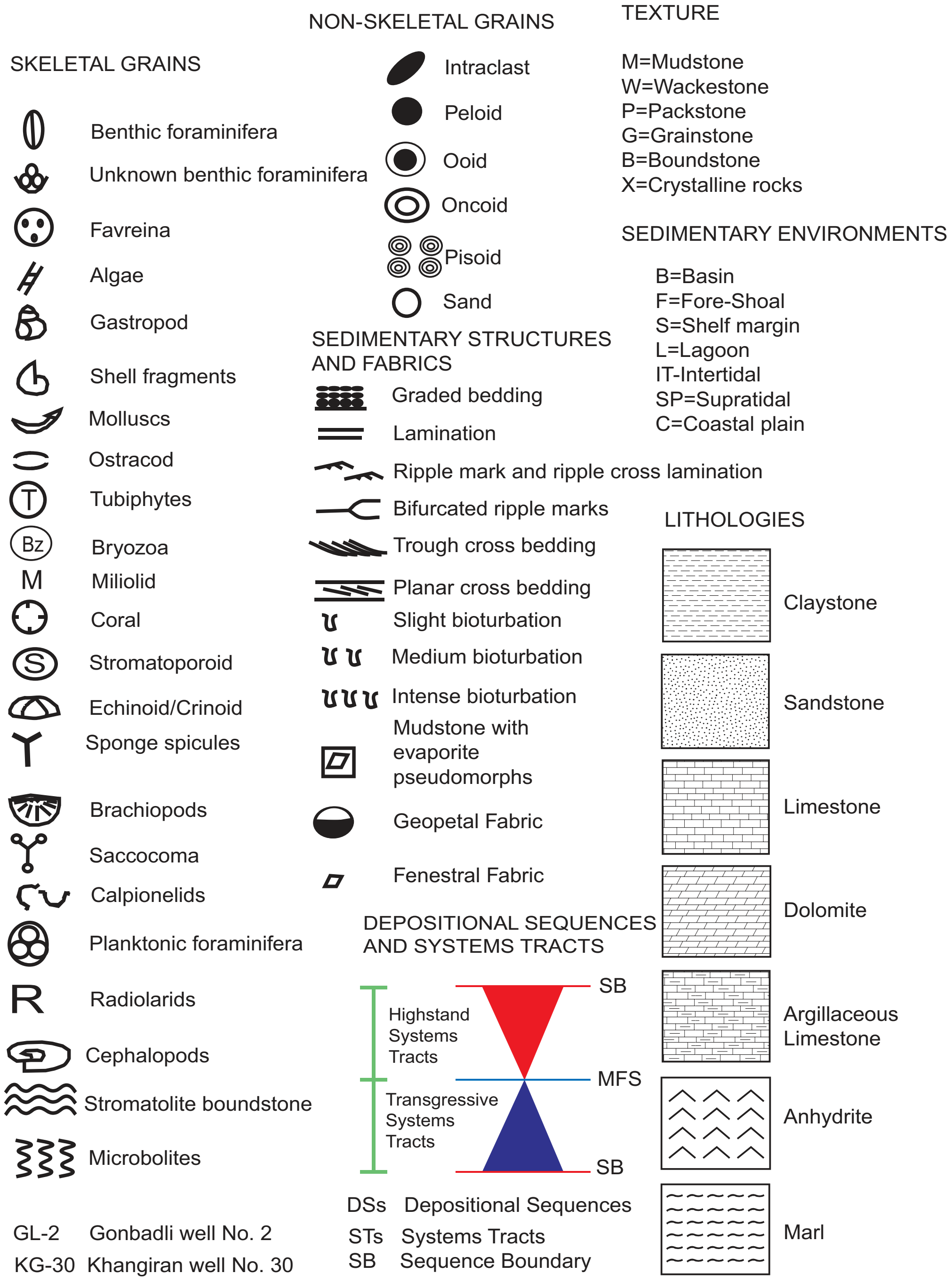

Table 2. Key to symbols and abbreviations used in measured sections and well logs (Figs 5-9).

grainstones are often thinner, less common and richer in oncoids (Della Porta *et al*., 2004). These deposits pass vertically into lime mudstones, dolomitized sandy ooid grainstone/packstones and *Tubiphytes* packstones. The MFS is indicated by bioclastic packstones with crinoid/echinoids and *Tubiphytes.*

The change from subtidal to mainly intertidal and supratidal conditions indicates sea-level fall and a reduction of accommodation during the HST. HST deposits in the subsurface at *Khangiran* and *Gonbadli* (Figs 8, 9) are characterized by progradation of fore-shoal facies on shelf-margin environments. Sea-level fall results in a decrease in space for carbonate-producing biota due to emergence of the carbonate platform (Berra, 2007). Tidal-flat dolomudstone and laminated lime mudstone/dolomudstones, deposited in a supratidal setting, occurred during the late HST at the outcrop locations (Figs 5, 6, 7). Dolomitized supratidal deposits with microbial mats, dissolution features, birds-eyes and calcite pseudomorphs after gypsum/anhydrite, which appear in the late HST especially at the outcrop locations, indicate subaerial exposure (Catuneanu *et al*., 2005).

The upper sequence boundary at the outcrop locations is type 1, but is type 2 in the subsurface at *Khangiran* and *Gonbadli*.

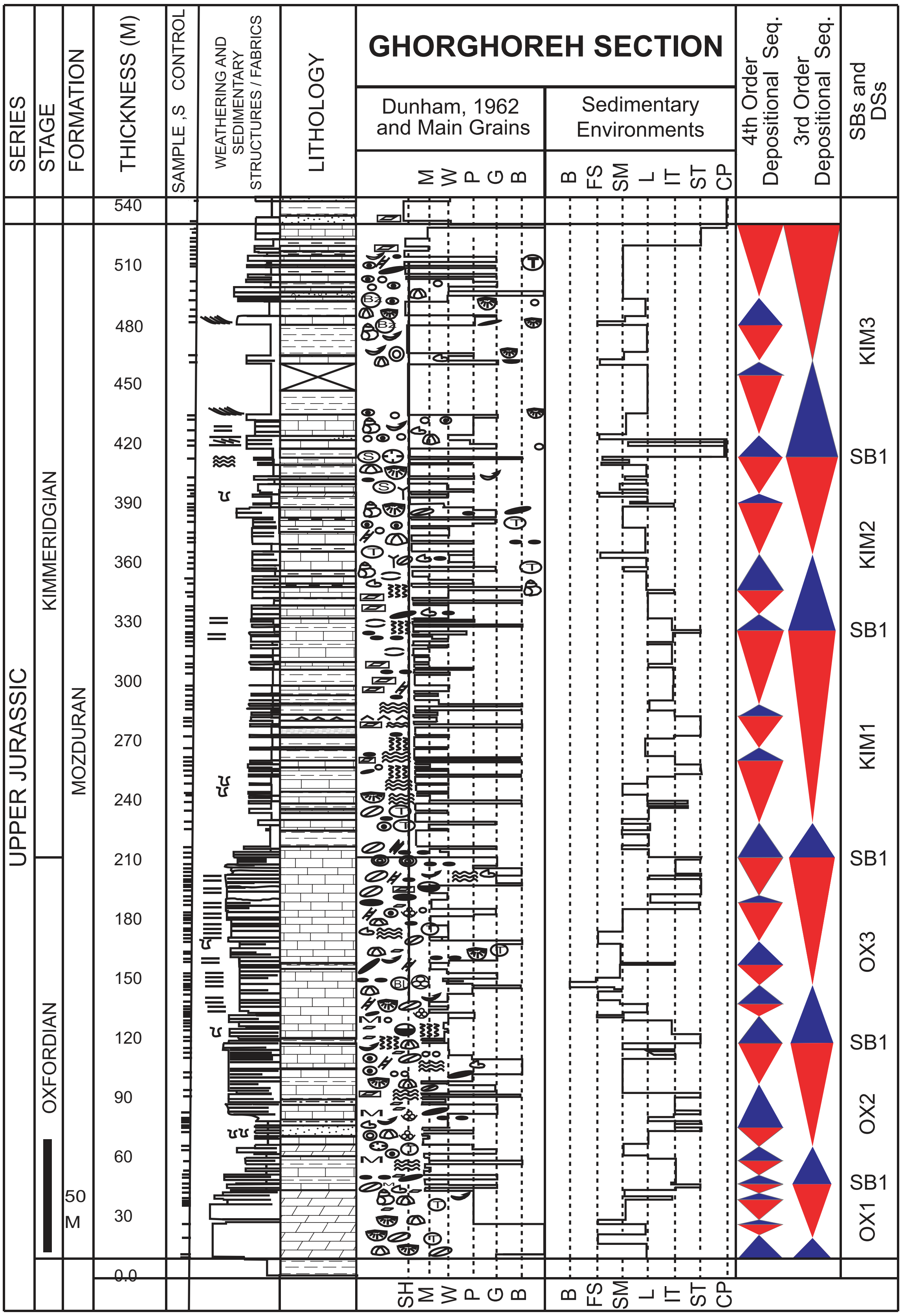

Fig. 5. Stratigraphy and depositional sequences (3rd and 4th order) of the Upper Jurassic Mozduran Formation at the Ghorghoreh outcrop (see Fig. 1 for location). Six depositional sequences (DSs) and related sequence boundaries (SBs) are identified. See Table 2 for symbols and abbreviations.

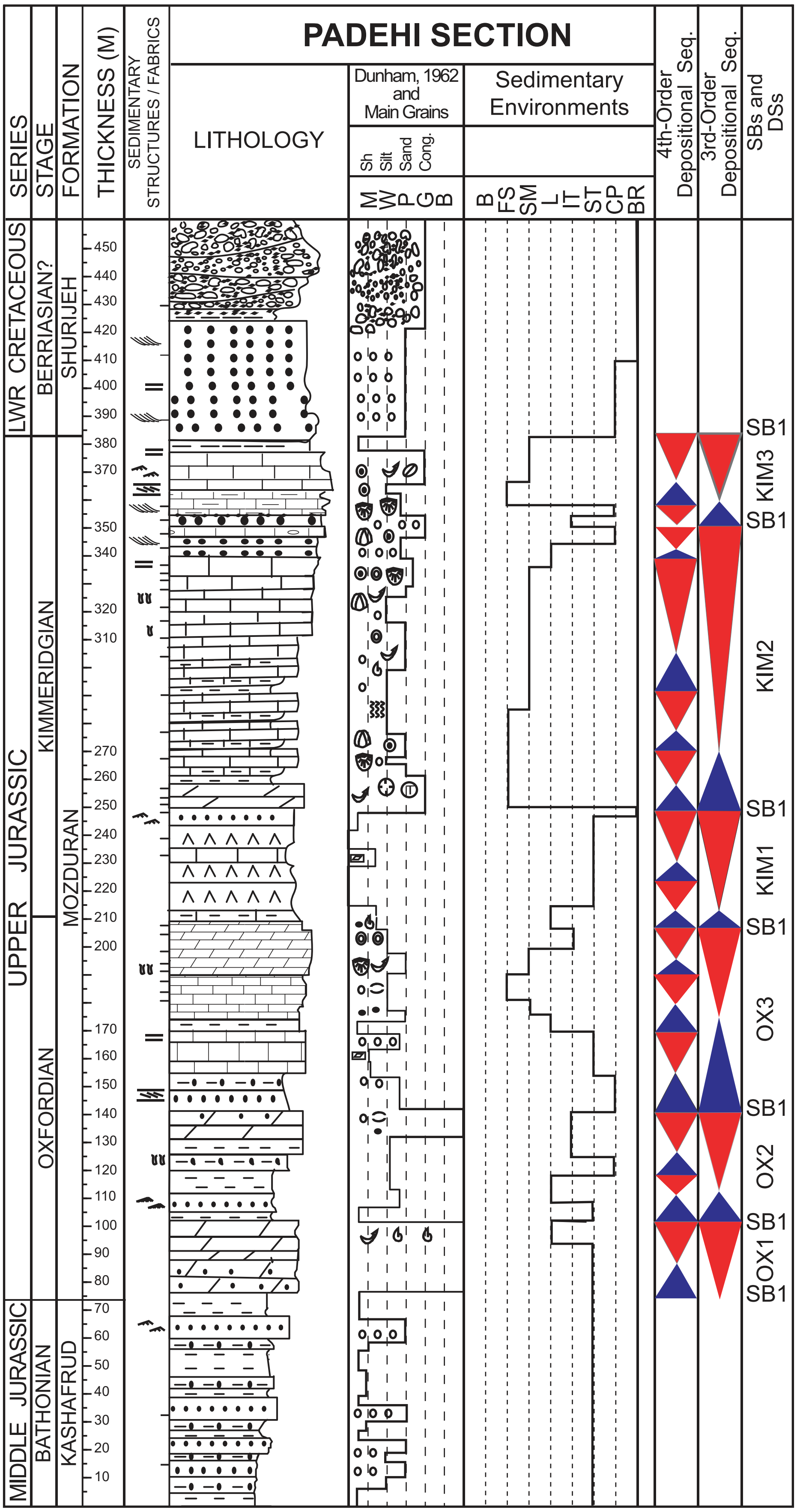

Fig. 6. Stratigraphy and depositional sequences (3rd and 4th order) of the Upper Jurassic Mozduran Formation at the Padehi outcrop (see Fig. 1 for location). Six depositional sequences (DSs) and related sequence boundaries (SBs) are identified. See Table 2 for symbols and abbreviations.

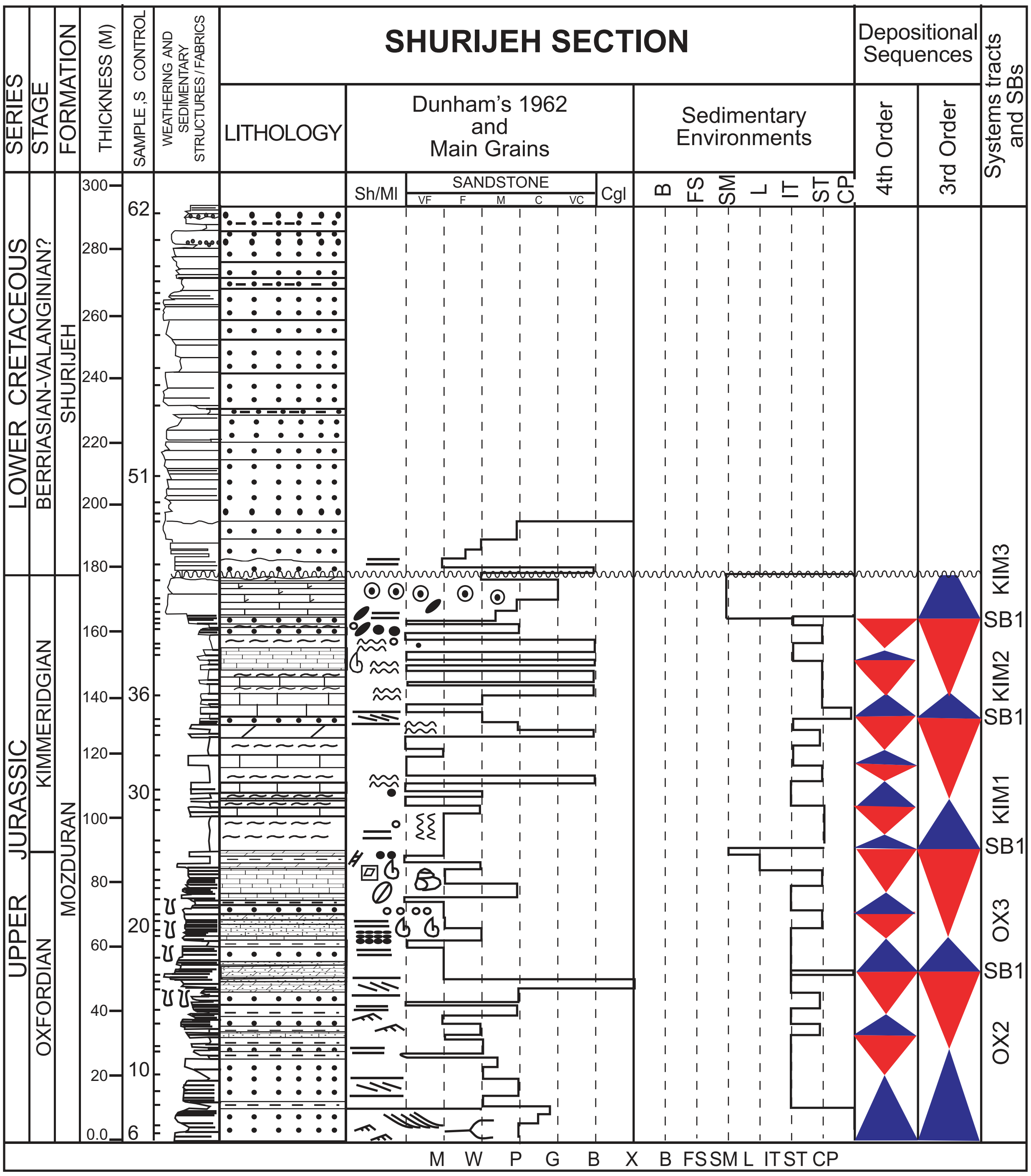

Fig. 7. Stratigraphy and depositional sequences (3rd and 4th order) of the Upper Jurassic Mozduran Formation at the Shurijeh outcrop (see Fig. 1 for location). Five depositional sequences (DSs) and related sequence boundaries (SBs) are identified. Sequence OX1 and the TST of OX2 were not deposited at this location. The HST of sequence KIM3 has been eroded. Thick siliciclastic deposits and relative thinning of the Mozduran Formation at this location indicate proximity to siliciclastic sources, a relatively elevated palaeotopographic position during deposition, and a low subsidence rate. See Table 2 for key to symbols and abbreviations.

3. Depositional Sequence 3: Oxfordian (OX3)

The boundary between sequences OX2 and OX3 is marked by significant deepening and consequently an clear shift in depositional environments. The transgressive systems tract in sequence OX3 include a range of depositional facies (shore face/tidal flat to basinal). At the Shurijeh surface section (Fig. 7), the transition from wave-rippled sandstones to current-rippled (tidal) sandstones to sandstones with a carbonate matrix and increasing carbonate layers together with marine fauna indicate a retrogradational stacking pattern. The transgressive systems tract in the western outcrops and gasfields is indicated by the occurrence of carbonates containing more normal marine fauna with a decrease and even absence of siliciclastics as a result of a general increase in accommodation.

The thickening of parasequences on an aggraded flat-topped platform is common in transgressive systems tracts (Goldhammer *et al*., 1991). The absence of shallow-water fauna and a high gamma-ray reading, together with the presence of sponge spicules, S*accocoma*, tintinnids, radiolarids and planktonic foraminifera at *Khangiran* and *Gonbadli* (Figs 8, 9) indicate the TST. Due to aggradation of pelagic facies at *Khangiran* and *Gonbadli*, we define a maximum flooding zone (MFZ) instead of a maximum flooding surface. The overall increase in accommodation towards the *Khangiran* and *Gonbadli* anticlines compared to the southern outcrops (Figs 10A, B) reflects tectonic subsidence. Large oncoids occur in TST deposits to the west of the Ghorghoreh section. These occur within onlapping packages which show backstepping platform facies (Whalen *et al*., 2002). The occurrence of benthic foraminifera a few metres above the MFZ (early highstand systems tract in sequence OX3) indicates gradual shallowing of the depositional environment as a result of progradation.

The early highstand systems tract in sequence OX3 is characterized by a proliferation of benthic organisms and consequently a sudden increase in carbonate content (Carpentier *et al*., 2007). HST deposits at the *Khangiran* and *Gonbadli* wells and surface sections represents a thickening- and coarsening-up interval with skeletal and non-skeletal grains which indicates high sediment production rates with progradation when sufficient accommodation space was available. Progradation of strata into the deep basin at the gasfields (Figs 8, 9) is inferred by the interfingering of pelagic facies with calciturbidites, which in turn are underlain by a fore-shoal and shelf-margin facies belt containing *Tubiphytes* packstone/boundstones, microbialite boundstones and bioclastic (*Nautiloculina oolithica*, *Cayeuxia*) peloid packstone facies, respectively. Progressive progradation is indicated by vertical thinning of pelagic intervals accompanied by the disappearance of gamma-ray peaks (Fig. 8). The presence of clinoforms in seismic images (see Figs 12, 13A) suggests progradation as a result of the high carbonate production rate.

Thicker limestones capping the cycles represent highstand deposits in a fore-shoal environment and are underlain by shallower-water carbonates, indicating that carbonate production and accumulation outpaced relative sea-level rise (Strasser *et al*., 1999). This depositional sequence is composed of tight, dense limestone as indicated from logs and confirmed by drill-stem tests.

The lower and upper sequence boundaries in the study area are type 1; however, the lower sequence boundary at *Khangiran* and *Gonbadli* is type 2 (Figs 8, 9).

4. Depositional Sequence 4: Kimmeridgian (KIM1)

This sequence contains the LST in the study area which is composed mainly of red marls and evaporites (Figs 6, 7). The transgressive systems tract shows a range of depositional environments from tidal flat to fore-shoal, and facies are composed mainly of green marls, bioclastic wackestones and stromatolite boundstones; marls decrease upwards. TST deposits are thin in southern outcrops of the study area (Figs 5, 6, 7).

The MFS at southern outcrop locations (Fig. 1) was indicated by facies evolution (i.e. the ratio of marl/limestone decreases upwards), and by a bed containing annelids, *Tubiphytes, Lithocodium* and brachiopods. The presence of annelids suggests low sedimentation rates characterizing the MFS. At the gasfields, the MFS is characterized by bioclastic wackestone containing sponge spicules and *Saccocoma*.

The HST at Ghorghoreh (Fig. 5) shows a progradational stacking pattern from lagoon to intertidal and then to supratidal sub-environments. The shallowing-upward trend from shoal/lagoonal to supratidal is indicative of a progradational stacking pattern during the highstand systems tract (Kwon *et al*., 2006). The repetition of laminated stromatolite boundstones and lime mudstone/dolomudstones with calcite pseudomorphs after gypsum/anhydrite and microbreccia in thin-bedded limestones with marl interbeds is interpreted to indicate progressive progradation during the late HST and a general loss in accommodation near the sequence boundary. Dolomitized supratidal deposits with microbial mats, dissolution features and birds-eyes indicate subaerial exposure (Catuneanu *et al*., 2005).

The occurrence of evaporites within supratidal deposits, or above subtidal deposits, indicates sea-level fall or progressive restriction related to sedimentary processes, such as barrier-bar construction (Lucia, 1999). High amounts of ostracods accompanied by calcite pseudomorphs after gypsum and micro-solution breccias in the KIM1 and KIM2 sequences at Padehi and Ghorghoreh indicate very shallow and restricted environments and arid conditions. Progradation during HST of KIM1 at the *Khangiran* and *Gonbadli* wells is indicated by a gradual transition from pelagic to fore-shoal, shelf margin, lagoon and tidal flat facies with anhydrite at Gonbadli as interpreted from density and high resistivity wireline log motifs (Figs 8, 9).

Pisoids at the Ghorghoreh and Shurijeh sections and at well *Gonbadli-2* were chosen as the upper boundary of the KIM1 sequence. Both lower and upper sequence boundaries are type 1.

5. Depositional Sequence 2: Kimmeridgian (KIM2)

At the *Gonbadli* structure, LST deposits in this sequence are composed of mixed siliciclastics and gypsum/anhydrite (Fig. 8). At *Khangiran*, the LST is indicated by thin marls/claystones (Fig. 9). At Ghorghoreh, the LST is represented by thick marls and at Padehi and Shurijeh it is composed of sandstones (Figs 6, 7). Symmetrical ripple-marks in sandstones at Padehi suggest wave activity in a shallow nearshore setting.

The transgressive systems tract includes a range of depositional facies from shoreface to fore-shoal. The presence of fine- to medium-grained sandstones early in the transgression may represent siliciclastic supply during times with little dilution by fine-grained carbonate sediment (Whalen *et al*., 2000). At outcrop sections, the TST is characterized by lime mudstones with fenestral fabrics, stromatolite boundstones to bioclastic wackestones and bioclastic packstones containing algae, *Tubiphytes*, echinoids, crinoids, gastropods, corals and brachiopods (Figs 5, 6, 7). The TST at the gasfields is characterized by *Tubiphytes* grainstones, dolomitized ooid grainstones (with isopachous cement), bioclastic wackestones and bioclastic packstones interpreted to indicate lagoonal to fore-shoal environments (Figs 8, 9).

In the well successions, the HST is indicated by widespread carbonate production and then slow carbonate production with siliciclastic input. The presence of vadose silt at *Khangiran-30* indicates a temperate climate and high rainfall. Sequence KIM2 serves as a reservoir unit at *Khangiran* and *Gonbadli*, and HST deposits are characterized by intense progradation (Figs 8, 9). Dolomitized ooid grainstones with blocky and poikilotopic fabrics and intercrystalline porosity reflect dolomitization; they suggest a general increase of carbonate production in the HST of this sequence in these wells. At *Gonbadli,* high resistivity and the density log motif indicate thick anhydrites. This is corroborated by core observations (Fig. 11). At Padehi, the HST thickens upwards and carbonate production is abruptly interrupted by siliciclastic input. The presence of thick, cross-bedded quartz arenites indicates a shore-face depositional environment. Stromatolite boundstones in the HST at Shurijeh (Fig. 7) are followed by thin sandstone beds. Dolomitized supratidal deposits with microbial mats, dissolution features, fenestrae and mud cracks indicate subaerial exposure (Catuneanu *et al*., 2005). In the upper interval, the presence of sandstone layers above thin carbonate packages (highstand systems tract) indicates a forced-regressive systems tract (c.f. Hunt and Tucker, 1993).

The presence of sandstones in the HST containing plant remains implies a climatic change from arid to temperate. This pattern has been recognized in depositional sequences that formed in tandem with 100 ka and 400 ka orbital cycles (Strasser *et al*., 1999). The upper boundary of the sequence at Padehi and Shurijeh is characterized by iron ooids. A continental origin for the iron ooids cannot be excluded because gastropod and crinoid fragments incorporated into the nuclei of the ooids show no evidence of erosion and abrasion.

The upper sequence boundary resulted from a fall in relative sea-level associated with a downward shift in facies (Figs 5, 6, 7). The lower and upper boundaries of the sequence are type 1 in the study area.

6. Depositional Sequence 3: Kimmeridgian (KIM3)

This sequence begins with a LST that is composed of lithic greywackes, siltstones, claystones and marls. Cross-bedded sandstones overlying marls represent the LST in the southern outcrops. At *Gonbadli*, the LST is composed mainly of gypsum/anhydrite with thin sandstone.

The transition from the KIM2 to the KIM3 sequence accompanied a major climate change from humid/temperate to arid conditions, as inferred from the transition of sandstones containing plant remains and iron ooids to evaporites and red sandstones and siltstones. The TST is composed of intraclastic grainstones, bioclastic wackestones and bioclastic packstones at *Khangiran* and *Gonbadli* (Figs 8, 9). The occurrence of more open-marine facies during the TST in this sequence is consistent with global sea-level rise during the Late Jurassic (Hallam, 1988; Haq *et al*., 1987). At the outcrops, a retrogradational stacking pattern is indicated by a lack of siliciclastics, thickening-up and vertical and lateral facies evolution from intraclastic packstone/grinstone, dolomitic/dolomitized ooid grainstone with quartz nuclei to the dominance of brachiopod packstones. At outcrops, the

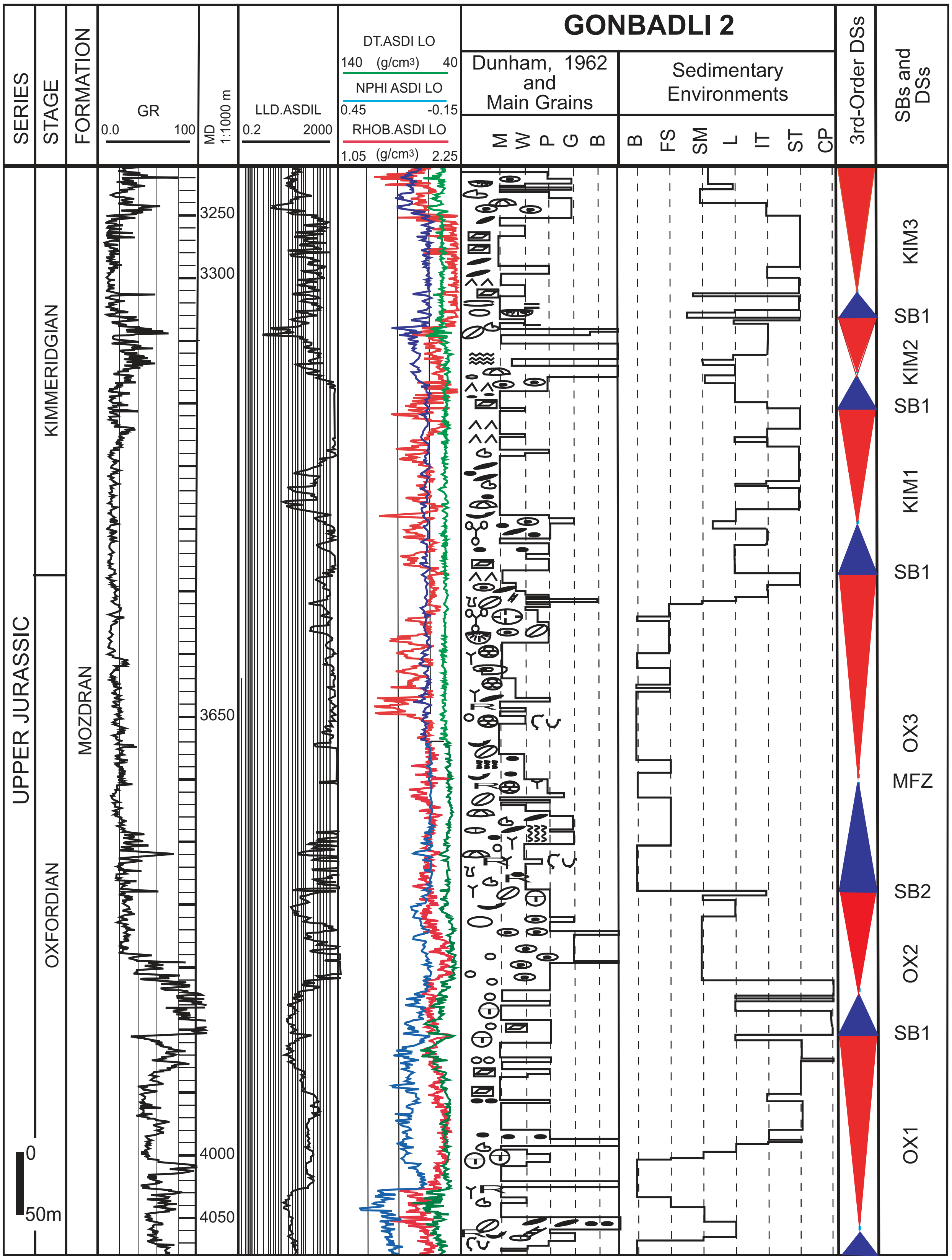

Fig. 8. Stratigraphy and depositional sequences of the Upper Jurassic Mozduran Formation in well *Gonbadli-2 (GL-2)*. Six depositional sequences (DSs) and related sequence boundaries (SBs) are identified. Depositional sequences OX2 and OX3 are composed of tight and dense carbonate as indicated from resistivity, density and neutron log motifs. The boundary between the OX3 and KIM1 depositional sequences is marked by an anhydrite interval as indicated by density and resistivity log motifs.

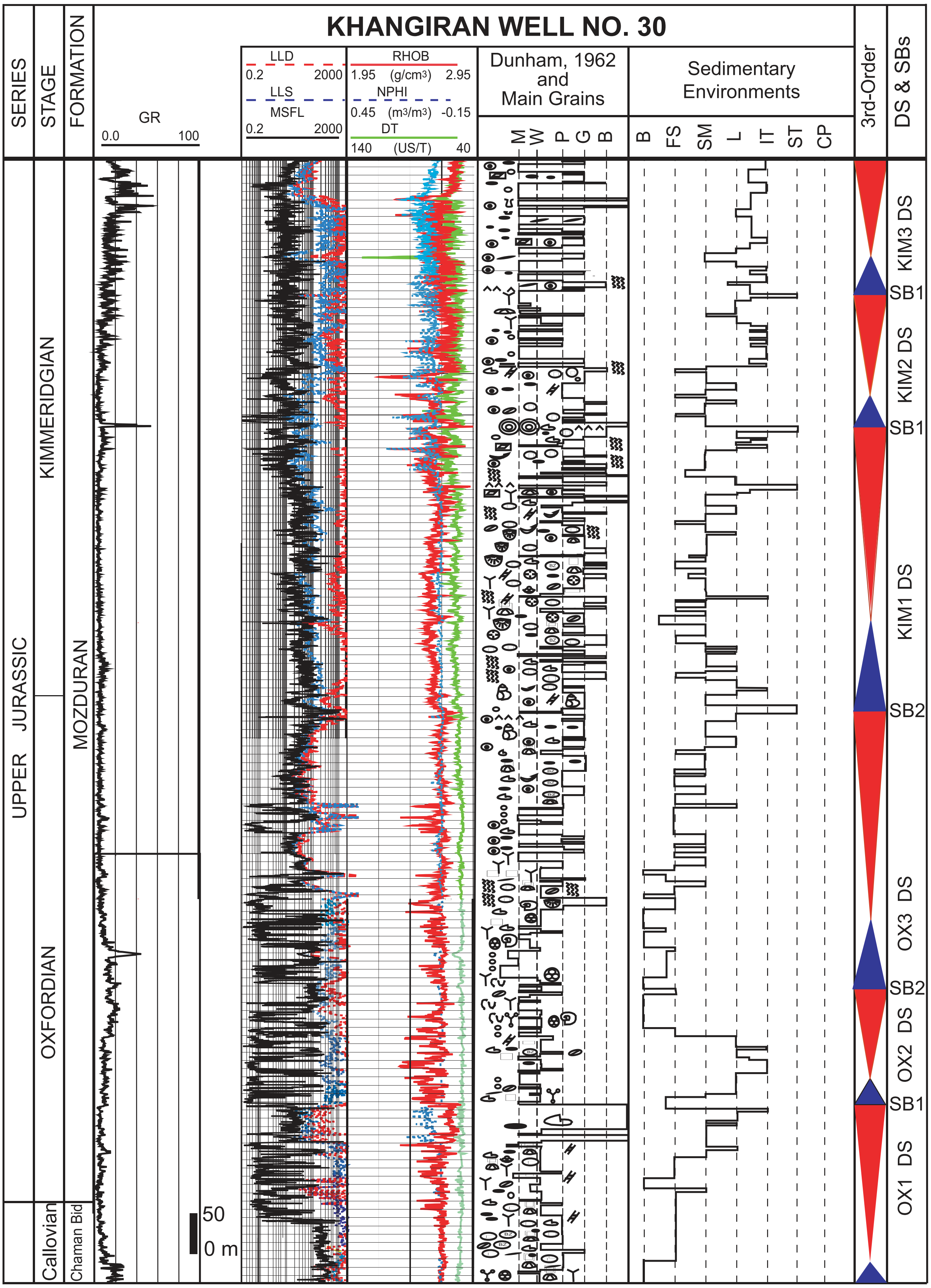

Fig. 9. Stratigraphy and depositional sequences of the Upper Jurassic Mozduran Formation in well *Khangiran-(KG) -30*. Six depositional sequences (DSs) and related sequence boundaries (SBs) are identified. Pay zones with good porosity occur in the KIM1 and KIM2 depositional sequences. The proximity of the neutron and density logs in dolomitized intervals is probably related to gas effects.

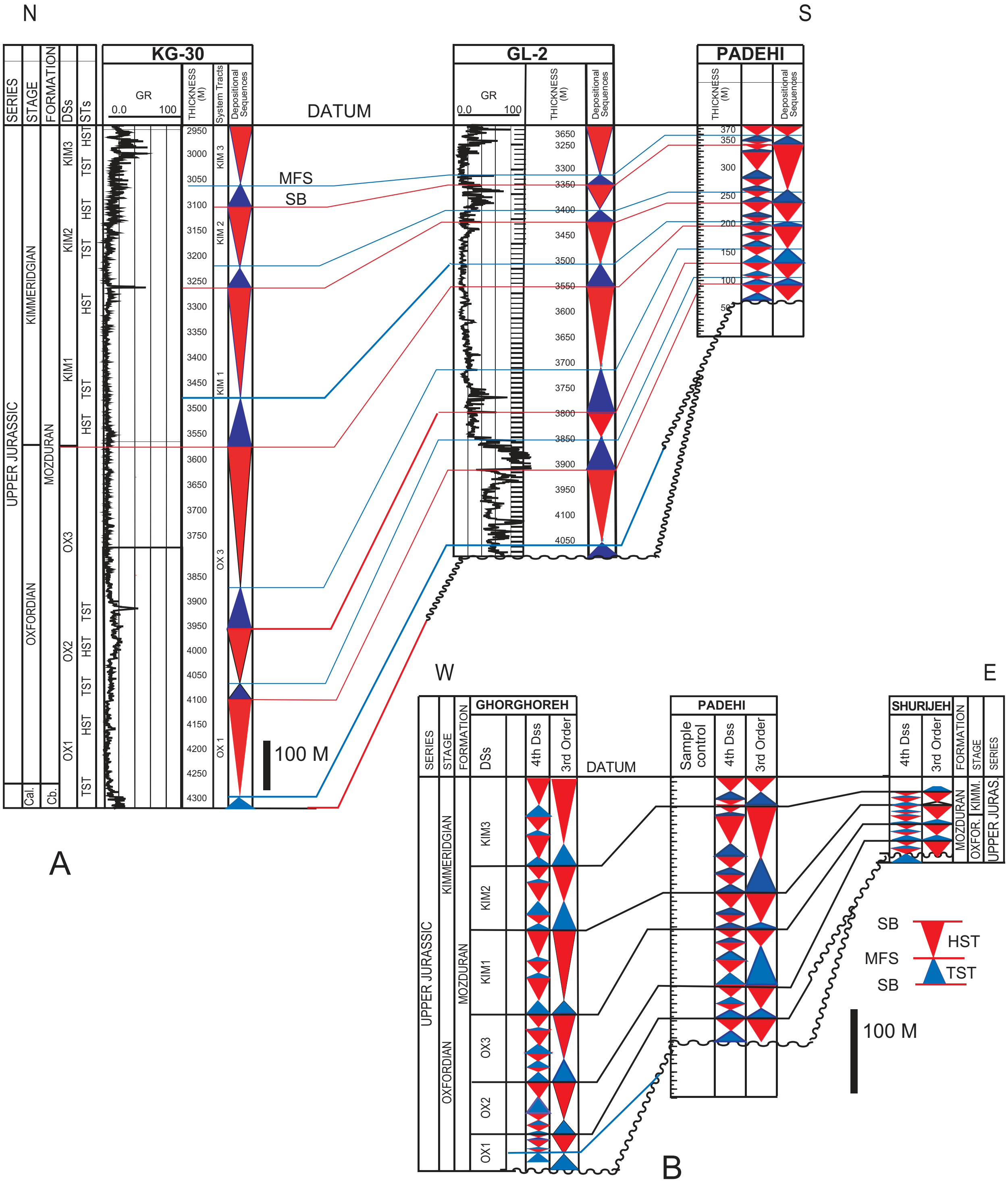

Fig. 10. (A) Correlation of depositional sequences along a profile from the Padehi surface section (south) to the *Gonbadli* and *Khangiran* gasfields in the north of the study area (see Fig. 1 inset locations). Note the thickness variations in the depositional sequences, which indicate a tectonic role in the control of depositional sequence variations. (B) East-west correlation of depositional sequences in the Mozduran Formation between the Shurijeh, Padehi and Ghorghoreh outcrop sections in the Kopet Dagh Mountains (see Fig. 1 for locations).

MFS is characterized by layers composed completely of brachiopods and in wells by sponge spicule wackestones.

During the HST, relatively high subsidence rates plus sea-level rise in the basin (i.e. in the north and west of the study area) resulted in very thick sediment accumulation. At *Khangiran-30* and *Gonbadli-2*, the HST is characterized by a transition from shelf margin to lagoonal and tidal flat facies. Dolomudstones and lime mudstones with evaporite casts appear in uppermost part of the Mozduran Formation. The abundance of ooid grainstones and tidal flat facies, together with evidence for exposure and vadose diagenesis (inferred from vadose silt, Fe-staining and fresh-water phreatic cement fabrics) indicates a marked decrease in accommodation, especially at the *Khangiran-30* location. The northern and western parts of the basin were not emergent but siliciclastic materials were probably supplied from the south during sea-level falls. Low angle depositional surfaces can result in significant facies shifts across medium-scale (4th-order) sequence boundaries (van Buchem *et al.,* 1996). At Shurijeh, the highstand systems tract is absent and has been eroded (Figs 5, 6, 7) during tectonic activity. Sea-level fall led to erosion of carbonate deposits, especially in the eastern parts of the Kopet Dagh Basin (Figs 10A, B).

FORMATION OF SEAWAYS

Seismic images (Fig. 12) and the analysis of depositional sequences indicate that, following maximum flooding during the late Oxfordian, a series of narrow seaways developed in the Kopet Dagh Basin. The rate of carbonate production was high enough in footwall locations to keep up with relative sea-level rise (Fig. 13A). This resulted in an aggradational stacking pattern on the platform. Aggradation on the platform margin and reduced carbonate production in the deep basin together with differential subsidence resulted in considerable palaeotopographic differentiation. In the deep basin, pelagic facies were deposited with little sediment supply during greater tectonic subsidence. Aggradation on the platform margin and reduced carbonate production in the deep basin together with differential subsidence resulted in the creation of narrow seaways during the late Oxfordian (Fig. 13A).

During the TST of sequence OX3, sea-level rise resulted in siliciclastics being pushed landward and in condensation of basinal deposits. Maximum sea-level rise is suggested by facies evolution and stacking patterns in the Kopet Dagh Basin during the late Oxfordian. The sea-level rise is confirmed by partial drowning of Oxfordian carbonates (Esfandiar Formation) in Central Iran, as indicated by condensed horizons and hardgrounds (Seyed-Emami *et al*., 2004).

Dark-coloured thin-bedded limestones and marls were deposited in the seaways and are referred to as the Chaman Bid Formation. The presence of calciturbidites within the pelagic facies confirms the seaward progradation of shallower depositional environments, which in turn were underlain by shallower-marine carbonates and evaporites (Fig. 13A) that are probably associated with the preservation of organic matter and formation of source rocks. The presence of oil stains in uppermost Kimmeridgian deposits and their absence in Oxfordian strata in the Mozduran Formation indicates that pelagic deposits may have source potential in the east of the Kopet Dagh Basin. Geochemical analyses have shown that the Chaman Bid Formation has sufficiently high TOC to produce hydrocarbons (Rashidi and Tarhandeh, 2007).

Interior seaways developed in back-arc settings are in general characterized by ramp-like profiles (Schwarz *et al*., 2006). In the study area, infilling of the deep basin adjacent to the carbonate platform by calciturbidites resulted in the transition from a rimmed shelf to a carbonate ramp (Figs 4B, 12, 13A, 13B). The ramp profiles became wider and smoother as the result of progressive progradation during the late Kimmeridgian. Thickening- and shallowing-upward trends in the northern part of the study area are due to filling of the seaways by progradation from the southern shallow-marine carbonate system.

The presence of more evaporites in some southern outcrops, porous carbonates in *Khangiran-30,* dense and impermeable carbonates in *Gonbadli-2* which are capped by evaporites (Fig. 11), may indicate the existence of stratigraphic traps. The system is sealed laterally by impermeable carbonates and on the other side by evaporites; meanwhile, the top of the sequence is indicated by gypsum/anhydrite at *Khangiran* and *Gonbadli*, respectively.

Towards the top of the Mozduran Formation succession (HST of the KIM2 and KIM3 sequences at Padehi, Ghorghoreh and *Khangiran-A*), reworking increases as a result of increasing occurrence of tempestites. Reworking increases upwards in the succession suggesting episodic high-energy storm events caused by a sea-level fall (Pawellek and Aigner, 2003). Climate change to more arid conditions resulted in gradual extinction of fauna and domination of non-skeletal grains and evaporites.

RESEVOIR QUALITY

The main hydrocarbon pay zones at the *Khangiran* and *Gonbadli* fields are located in the HSTs in sequences KIM1 and KIM2. The occurrence of prolific reservoirs in highstand systems tracts have been reported in Cenomanian carbonates (Sarvak Formation) in the Zagros Basin in the SW Iran (Kavoosi and Lasemi, 2005). In the Mozduran Formation, reservoir facies are composed of *Tubiphytes* boundstones, *Tubiphytes* packstones and grainstones, microbialite boundstones, dolomitized ooid grainstone/packstones and dolostones. The aggregagation of these facies with corals in some intervals, cemented by marine cements with isopachous, fibrous and acicular fringe fabrics,

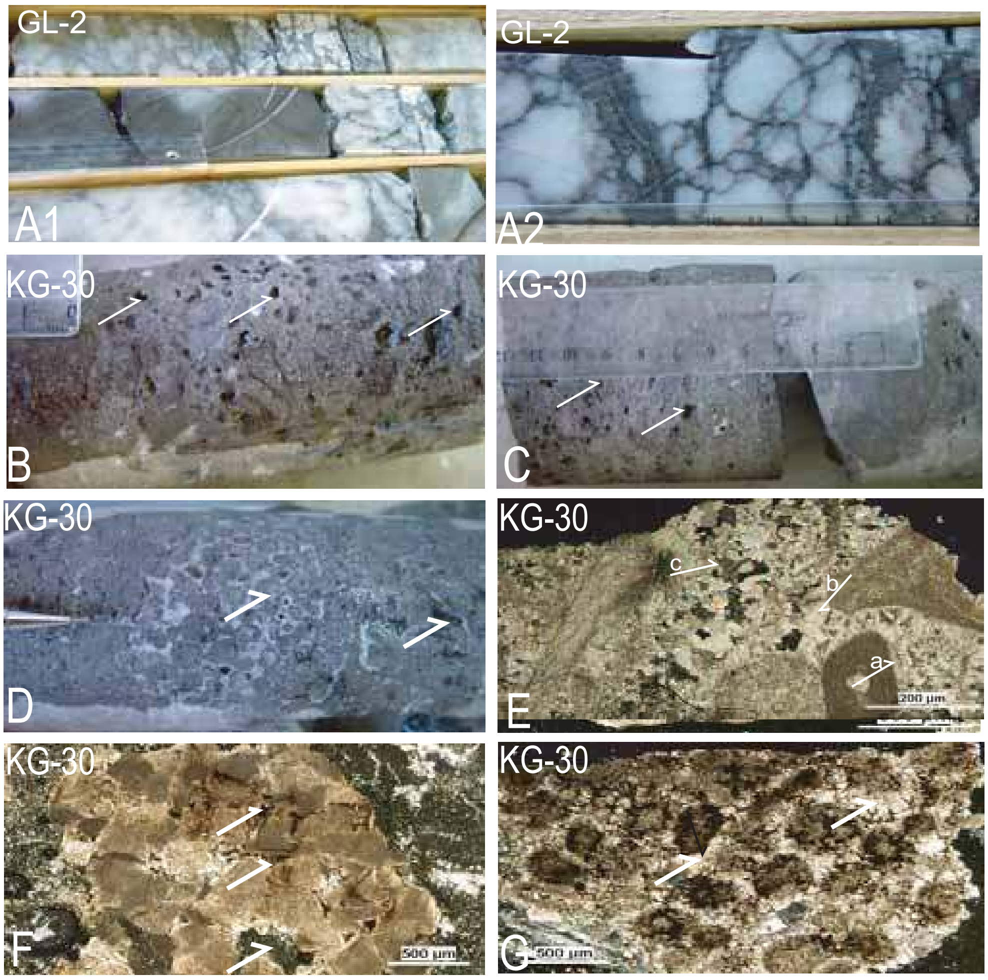

Fig. 11. (A) Core photograph of the Mozduran Formation in well *Gonbali-2*, depth 10,941-10,950 ft. Cores show four parasequences, the first of which begins with subtidal lime mudstone-wackestone followed by thick anhydrite capped by nodular anhydrite.
(B) Vuggy porosity (arrows) in the Mozduran Formation resulting from the dissolution of high-Mg calcite/ aragonite and dolomitization. Well *Khangiran 30,* depth 3217.5 - 3217 m.
(C) Facies controlled dolomitization in the Mozduran Formation with good porosity (arrows). Well *Khangiran 30*, depth 3217 - 3216.5 m.
(D) Coarse-grained ooid grainstone in the Mozduran Formationwith interparticle and dissolution porosity (arrows). Well *Khangiran 30*, depth 3217-3216.5 m.
(E) Thin section of bioclastic grainstone in the Mozduran Formation with two generations of cement: isopachous marine cement and drusy mosaic calcite cement which formed in the fresh-water phreatic zone. *Khangiran 30*, depth 3240-3042m, PPL.
(F) Dolostone with intercrystalline porosity which has resulted from dolomitization and the prior dissolution of grains in the Mozduran Formation. *Khangiran 30*, depth 3284-3286 m, PPL.
(G) Dolomitized ooid grainstone with equant and blocky cements. Cements have been dolomitized. *Khangiran 30,* depth 3206-3208 m, PPL.

indicate the presence of a reef on a windward margin and the high permeability of sediments at the *Khangiran-30* well location.

Petrographic analyses and wireline log motifs indicate that reservoir quality was controlled by depositional facies and diagenetic processes including dolomitization (Figs 8, 9,11). Dolomitization and intercrystalline porosity increase upwards in the succession (late HST) especially where anhydrites cap the parasequences. The presence of marine cements, vadose silts and acicular fringe aragonitic cements, and their absence at *Gonbadli-2,* indicate that *Khangiran-30* was in a relatively elevated palaeogeographic location during deposition of this sequence. Vadose silts and acicular fringe cements are rare during aggradation and are more common during progradation (e.g. Della Porta *et al*., 2004).

Petrographic studies indicate that Oxfordian ooids in the Mozduran Formation have preserved their radial and concentric fabrics, indicating that their primary mineralogy was composed of low-Mg calcite (LMC). However, Kimmeridgian ooids show both original aragonite and high-Mg calcite mineralogies which have been completely dolomitized so the original

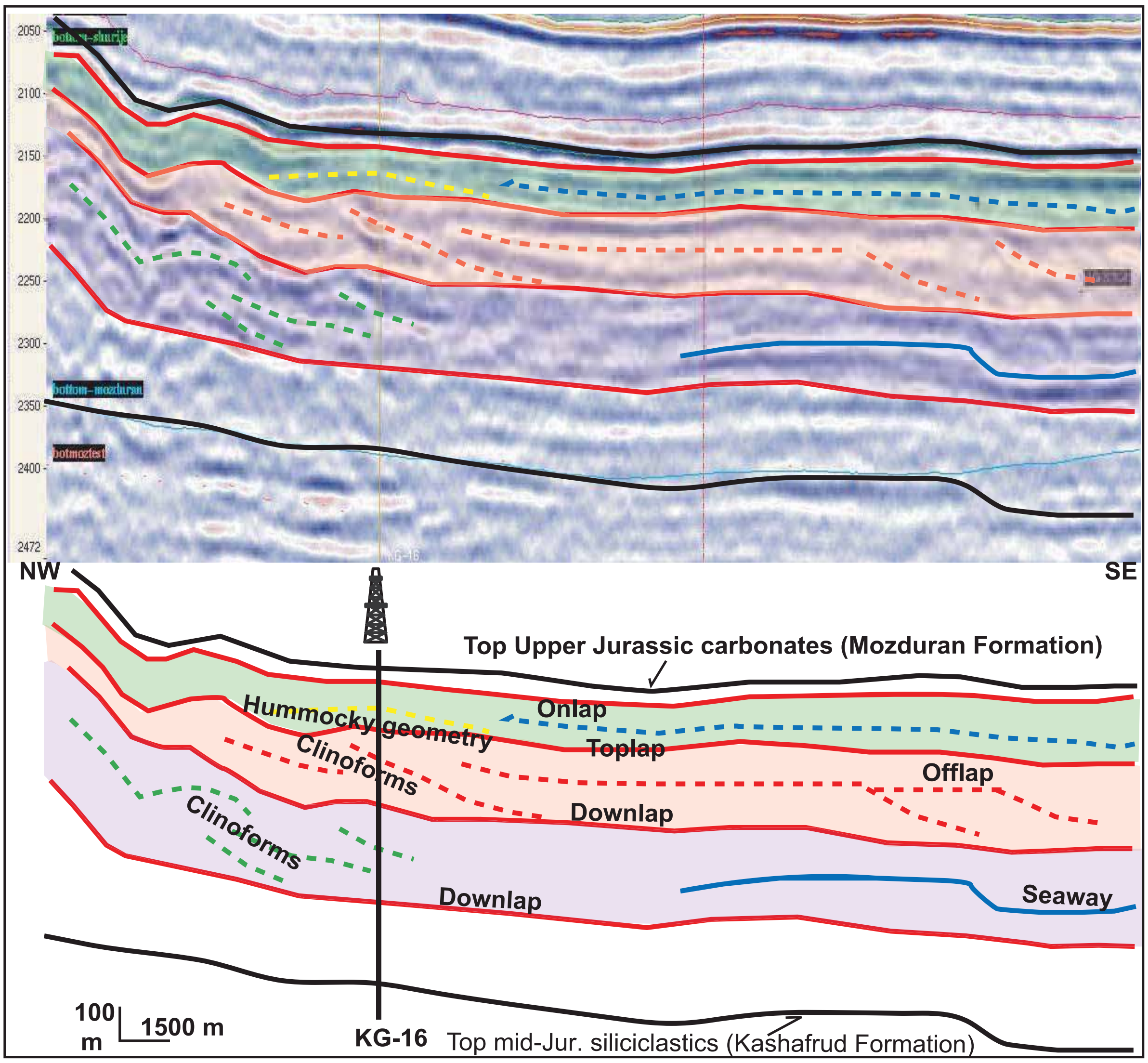

Fig. 12. NW-SE seismic profile across the *Khangiran* field, Kopet Dagh Basin, showing the Upper Jurassic Mozduran Formation. Seismic reflections indicate downlap towards the eastern part of the field and the presence of a seaway towards the right-hand end of the profile. The next phases of stratigraphic development were characterized by toplap and offlap, and then onlap, respectively. The image shows carbonate platform evolution from a rimmed shelf to a ramp during the Late Jurassic. See Fig. 1 for profile location.

fabric has been destroyed, although ghosts of spherical shapes remain. At *Khangiran* and *Gonbadli*, ooids in both the KIM2 and KIM3 sequences are aragonitic. Although ooids have been dolomitized, marine cements in the KIM1, KIM2 and KIM3 sequences at *Khangiran-30* show excellent preservation. Some cements (isopachous) show mimetic dolomitization. Preservation of the original aragonitic fabric of the cement suggests that dolomitization took place before aragonite inversion to calcite (Corsetti *et al*., 2006). At *Khangiran-30*, reefs/patch reefs developed in the KIM1 sequence. Increased hypersalinity, evaporite precipitation and consequently an increase in the Mg/Ca ratio, along with increasing high temperature (inferred from increasing evaporites), led to the preferential formation of aragonite to calcite. The aragonite mineralogy could be a result of evaporite precipitation and consequently an increase in Mg/Ca ratio; a high Mg/Ca ratio is thought to favour aragonite seas (Hardie, 1996; Stanley and Hardie, 1998). The presence of preserved ooids with radial and concentric cortexes in shallow-water settings which are near to a siliciclastic source, together with the formation of aragonitic ooids accompanied with evaporites in the gasfields, suggest that the mineralogy was probably controlled by salinity variations.

DISCUSSION

Correlation of depositional sequences (Figs 10A, B) draws attention to distinct changes in facies and patterns of retrogradation / progradation within each

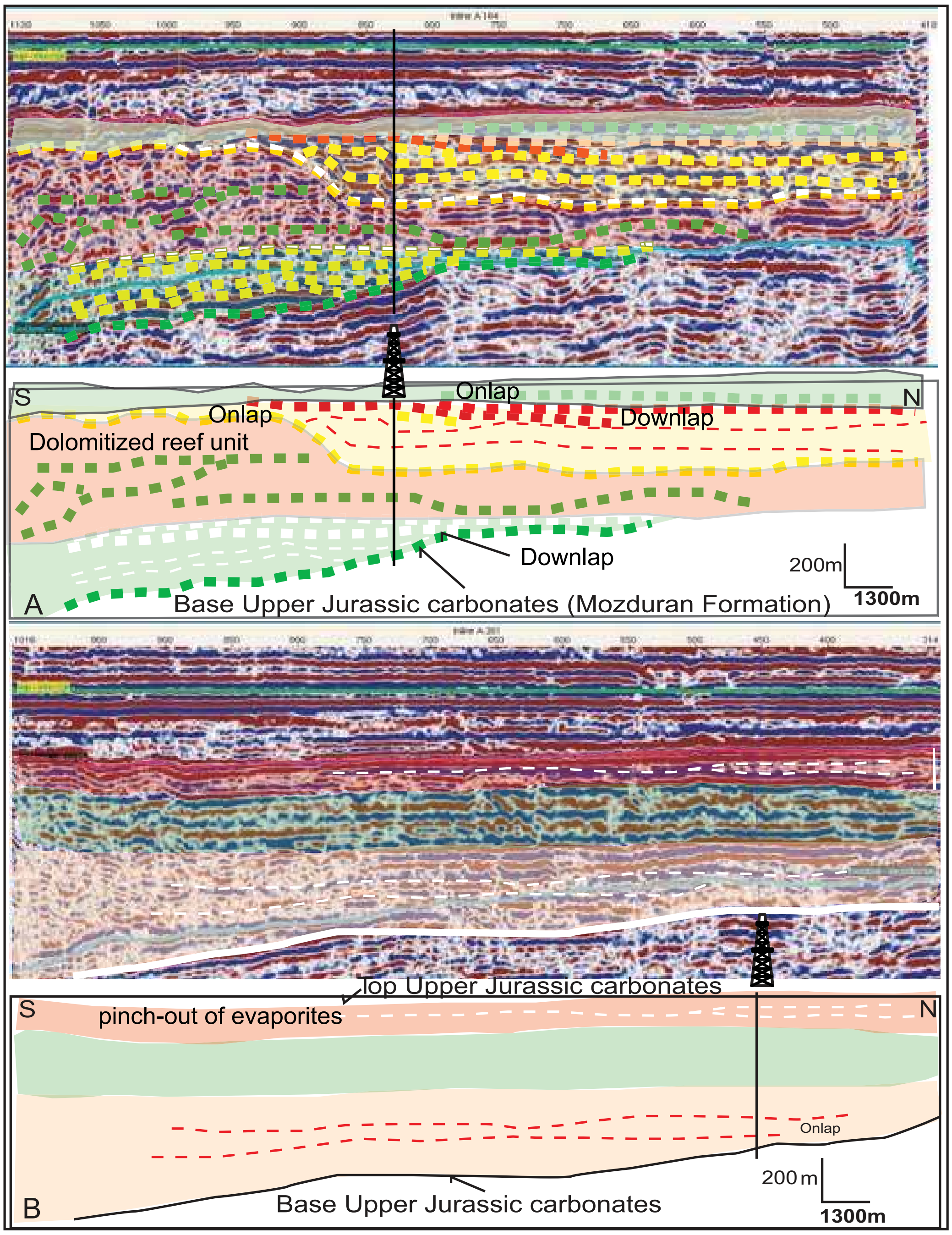

Fig. 13. Seismic profiles across the *Khangiran* (A) and *Gonbadli* (B) fields in the Kopet Dagh Basin (see profile locations in Fig. 1). (A) The lower part of this profile indicates onlap of pelagic facies onto inherited palaeotopography. In the middle part, seismic reflections most likely indicate dolomitized intervals, followed by the establishment of a rimmed shelf. Differential subsidence together with higher carbonate production resulted in a higher topographic position on the platform, followed by onlap towards the south. (B) The lower part of this profile indicates onlap of pelagic facies onto inherited palaeotopography. In the upper part, seismic reflections show the pinch-out of evaporites towards the north.

systems tract. High subsidence rates towards the west and north are inferred from thickness variations, which have been balanced by varying accommodation rates. The OX3 sequence indicates an obvious change in the sedimentary system and maximum accommodation space creation, as a result of relative sea-level rise accompanied by tectonic subsidence in the Kopet Dagh Basin. This sequence shows maximum landward migration of sedimentary environments, together with maximum development of reefal/bioclastic barriers on the shelf margin and platform top. The basinal thin-bedded limestones and marls deposited in seaways were deposited near to the shallow carbonate platform. The presence of oil stains in uppermost Kimmeridgian deposits and their absence in Oxfordian sediments of the Mozduran Formation indicate that these pelagic facies should be considered as potential source rocks.

Sequence boundaries in the Mozduran Formation are attributed to sea-level changes induced both by tectonic subsidence and sediment loading. Together with relative sea-level changes and the occurrence of arid conditions, tectonism played a major role in the spatial distribution of reservoir facies as a result of diagenetic processes. During overall regression in the Kimmeridgian, high quality reservoir facies (reefs and dolomitized packstones/grainstones) with limited lateral and vertical distribution were developed, for example in the *Khangiran* gasfield. Rapid lateral thickness variations of depositional sequences together with abrupt facies and thickness changes at *Khangiran* and *Gonbadli* (Figs 10, 13) indicate that tectonic factors have controlled reservoir configuration. The OX1 sequence, however, is composed mainly of dolostones with good intercrystalline porosity (Figs 8, 9) but no hydrocarbons have yet been tested in drilled wells. The OX2 and OX3 sequences are composed of dense limestones as indicated by resistivity, neutron and density logs (Figs 8, 9).

The sedimentary and tectonic evolution of the Kopet Dagh Basin was shaped during the Middle Jurassic. Onlap of pelagic facies onto inherited topography, as seen in seismic images (Figs 13A, 13B), and the pinch-out of evaporites towards the south of the study area (Fig. 13B), indicate a tectonic influence on the distribution of facies and depositional sequences. Differential palaeotopographic development during sedimentation controlled the spatial distribution of reservoir facies. This led to compartmentalization of the Mozduran Formation reservoir and the possible creation of stratigraphic traps, for example at *Khangiran*.

CONCLUSIONS

Upper Jurassic deposits of the Mozduran Formation in the Kopet Dagh Basin are composed of six depositional sequences. Sequence boundaries are attributed to sea-level changes induced both by tectonic subsidence and sediment loading. The main hydrocarbon pay zones at the *Khangiran* and *Gonbadli* fields occur in the HST of the Kimmeridgian 1 and 2 sequences. Reservoir quality has been controlled by both facies (reefs/patch reefs, packstone/grainstone) and diagenetic processes such as dolomitization, marine cementation and freshwater-induced solution of aragonitic and high-Mg calcitic grains. Thickness variations of sedimentary units together with abrupt facies changes from good reservoirs to dense and non-reservoir facies at the *Khangiran* and *Gonbadli* structures indicate the importance of tectonism in controlling the reservoir configuration.

ACKNOWLEDGEMENTS

The authors thank the National Iranian Oil Company Exploration Directorate (NIOCEXP) staff for permission to publish this paper, particularly M. Mohaddes, M. Zadehmohammadi and D. Baghbani for their support. We acknowledge colleagues from NIOCEXP particularly A. Feizi, E. Madani, N. Shokrzadeh and F. Taati for their assistance during field trips. M.A.K. acknowledges the late M. Sepehr for helpful discussions, and Sh. Javadian and H. Assilian for helpful suggestions. The comments of reviewers Frans van Buchem (*Maersk*) and Giancarlo Rizzi (*Task Geoscience*) on a previous version are acknowledged with thanks.

REFERENCES

ADABI, M.H. and RAO, C.P., 1991. Petrographic and geochemical evidence for original aragonite mineralogy of Upper Jurassic Carbonates (Mozduran Formation), Sarakhs area, Iran. *Sedimentary Geology*, **72**, 253-267.

AFSHAR-HARB, A., 1969. A brief history of geological exploration and geology of the Sarakhas area and the Khangiran gas field. *Bulletin of the Iranian Petroleum Institute* **37**, 86 pp (in Persian).

AFSHAR-HARB, A., 1979. The stratigraphy, tectonics and petroleum geology of the Kopet Dagh region, northern Iran. Unpublished Ph.D thesis, Imperial College of Science and Technology, London, 316pp.

AFSHAR-HARB, A., 1982. Geological quadrangle map of Sarakhs, 1:250,000 scale (one sheet). Exploration and Production, NIOC, Tehran.

AGHANABATI, A., 2004. Geology of Iran. Geological Survey of Iran publication, 558 pp (in Persian).

AIGNER, T., 1982. Calcareous tempestites: storm–dominated stratification, Upper Muschelkalk limestones (Middle Triassic, SW Germany). In: EINSELE, G. and SEILACHER, A., (Eds), Cycles and events in stratigraphy. Springer-Verlag, Berlin, 180-198.

AIGNER, T., 1985. Storm depositional systems. Springer-Verlag, Berlin, 174pp.

ALAVI, M., 1991. Sedimentary and structural characteristics of the Paleo–Tethys remnants in northeastern Iran. *GSA Bull.*, **103**, 983-992.

ALAVI, M., VAZIRI, H., SEYED-EMAMI, K. and LASEMI, Y., 1997. The Triassic and associated rocks of the Aghdarband areas in central and northeastern Iran as remnant of the southern Turanian active continental margin. *GSA Bull.*, **109**, 1563-1575.

ALLEN, B., VINCENT, S.T., ALSOP, G.I., ISMAIL-ZADEH, A. and FLECKERD, R., 2003. Late Cenozoic deformation in the South Caspian region. Effects of a rigid basement block within a collision zone. *Tectonophysics*, **366**, 223-239.

BERRA, F., 2007. Sedimentation in shallow to deep water carbonate environments across a sequence boundary: effects of a fall in sea-level on the evolution of a carbonate system (Ladinian-Carnian, eastern Lombardy, Italy). *Sedimentology*, **54**, 721-735.

BRUNET, M.F., KOROTAEV, M.V., EROSHOV, A.V. and NIKISHIN, A.M., 2003. The South Caspian Basin: a review of its evolution from subsidence modeling. *Sedimentary Geology*, **156**, 119-148.

BURYAKOVSKY, L.A., CHILINGER, G.V. and AMINZADEH, F., 2001. Petroleum geology of the South Caspian Basin. Gulf

Professional Publishing USA, 442pp.
CABIOCH, G., CAMOIN, G., WEBB, G.E., CORNEC, F.L., MOLINA, M.G., PIERRE, C. and JOACHIMSKI, M.M., 2006. Contribution of microbialites to the development of coral reefs during the last deglacial period. Case study from Vanuatu (South-West Pacific). *Sedimentary Geology*, **185**, 297-318.
CARPENTIER, C., LATHUILIERE, B., FERRY, S. and SAUSSE, J, 2007. Sequence stratigraphy and tectonosedimentary history of the Upper Jurassic of the Eastern Paris Basin (Lower and Middle Oxfordian, Northeastern France). *Sedimentary Geology*, **197**, 235-266.
CATUNEANU, O., MARTIN-NETO, M.A. and ERIKSON, P.G., 2005. Precambrian sequence stratigraphy. *Sedimentary Geology*, **176**, 67-95.
CHAFETZ, H.S., 1986. Marine peloids: a product of bacterially induced precipitation of calcite. *Sedimentary Petrology*, **56**, 812-817.
CHAFETZ, H.S., ALICIA, A., IMERITO-TETZALFF, J. and ZHANG, J, 1999. Stable-isotope and elemental trends in Pleistocene sabkha dolomites: descending meteoric water vs. sulfate reduction. *Journ. Sedim. Research*, **69**, 256-266.
CORSETTI, F.A., KIDDER, D.L. and MARENCO, P.T., 2006. Trends in oolite dolomitization across the Neoprotozoic-Cambrian boundary: A case study from Death Valley, California. *Sedimentary Geology*, **191**, 135-150.
DELLA-PORTA, G., KENTER, J.A.M., BAHMONDE, J.R., IMMENHAUSER, A. and VILLA, E., 2004. Microbial boundstone dominated carbonate slope (Upper Carboniferous, N Spain) facies, lithofacies distribution and stratal geometry. *Facies*, **49**, 175-208.
DICKSON, J.A.D., 1965. A modified staining technique for carbonates in thin section. *Nature,* **205**, 587.
DUNHAM, R.J., 1962. Classification of carbonate rocks according to depositional texture. In: Ham, W.E., (Ed.), Classification of carbonate rocks. *AAPG Mem.* **1**, 108-121.
EL-AZABI, M.H. and EL-ARABY, 2007. Depositional framework and sequence stratigraphic aspects of the Coniacian-Santonian mixed siliciclastic/carbonate Matulla sediments in Nezzazat and Ekma blocks, Gulf of Suez, Egypt. *Journal of African Earth Sciences*, **47**, 179-202.
EL-TABAKH, M., MORY, A., SCHREIBER, B.C. and YASIN, R., 2004. Anhydrite cements after dolomitization of shallow marine Silurian carbonates of the Gascoyne Platform, Southern Carnarvon Basin, Western Australia. *Sedimentology Geology*, **164**, 75-87.
FLÜGEL, E., 1982. Microfacies analysis of limestones. Springer-Verlag, Berlin, 633pp.
FLÜGEL, E., 2004. Microfacies of carbonate rocks. Springer-Verlag Berlin Heidelberg, 996pp.
GARZANTI, E. and GAETANI, M., 2002. Unroofing history of late Paleozoic magmatic arcs within the Turan Plate (Tuarkyr, Turkmenistan). *Sedimentary Geology*, **151**, 67-87.
GOLDHAMMER, R.K., DUNN, P.A. and HARDIE, L.A., 1991. Depositional cycles, composite sea-level changes, cycle stacking patterns, and hierarchy of stratigraphic forcing: examples from Alpine Triassic platform carbonates. *GSA Bull.*, **102**, 535-562.
GOLONKA, J, 2004. Plate tectonic evolution of the southern margin of Eurasia in the Mesozoic and Cenozoic. *Tectonophysics*, **381**, 235-273.
GRADZINSKI, M., TYSZKA, J, UCHMAN, A. and JACH, R., 2004. Large microbial-foraminiferal oncoids from condensed Lower-Middle Jurassic deposits: a case study from the Tatra Mountains, Poland. *Palaeogeography, Palaeoclimatology, Palaeoecology*, **213**, 133-151.
HANDFORD, C.R. and LOUCKS, R.G., 1993. Carbonate depositional sequences and systems tracts - responses of carbonate platforms to relative sea–level changes. In: LOUCKS, R.G. and SARG, J.F., (Eds), Carbonate sequence stratigraphy. *AAPG Mem.*, **57**, 3–43.
HAQ, B.U., 1991. Sequence stratigraphy, sea level change, and significance for the deep sea. In: Macdonald, D.I.M., (Ed.): Sedimentation, tectonics and eustasy. *Int. Assoc. Sedimentol. Spec. Publ.*, **12**, 3-39.
JACKSON, J, PRIESTLEY, K., ALLEN, M. and BERBERIAN, M., 2002. Active tectonics of the South Caspian Basin. *Geophysical Journal International*, **148**, 214-245.
HALLAM, A., 1988. A reevaluation of Jurassic eustasy in the light of new data and the revised Exxon curve. In: WILGUS, C.K., HASTINGS, B.S., POSAMENTIER, E., VAN WAGONER, J, ROSS, C.A. and KENDALL, C.G.St.C., (Eds): Sea-level changes: An integrated approach, *SEPM Special Publication*, **42**, 261-273.
HANDFORD, C.R. and LOUCKS, R.G., 1993. Carbonate depositional sequences and systems tracts - responses of carbonate platforms to relative sea–level changes. In: Loucks, R. G. and Sarg, J.F. (Eds), Carbonate sequence stratigraphy: recent developments and applications. *AAPG Memoir* **57**, 3-42.
HAQ, B.U., 1991. Sequence stratigraphy, sea-level change, and significance for the deep sea. In: Macdonald, D.I.M., (Ed.): Sedimentation, tectonics and eustasy. *Int. Assoc. Sedimentol. Spec. Publ.*, **12**, 3-39.
HAQ, B.U., HARDENBOL, J and VAIL, P.R., 1987. Chronology of the fluctuating sea-levels since Triassic. *Science*, **235**, 1156-1167.
HARDIE, L.A., 1996. Secular variation in seawater chemistry; an explanation for the coupled secular variation in the mineralogy of marine limestones and potash evaporites over the past 600 M.Y. *Geology*, **24**, 279-283.
HUNT, D. and TUCKER, M.E., 1993. Sequence stratigraphy of Carbonate shelves with an example from the mid-Cretaceous (Urgonian) of southeast France. In: POSAMENTIER, H.W., SUMMERHAYES, C.P., HAQ, B.U. and ALLEN, G.P., (Eds): Sequence stratigraphy and facies associations. Blackwell Scientific Publications, Oxford, 307-341.
HUSINEC, A. and READ, F., 2007. The Late Jurassic Tithonian, a greenhouse phase in the Middle Jurassic-Early Cretaceous "Cool" mode: evidence from the cyclic Adriatic platform, Croatia. *Sedimentology*, **54**, 317-337.
KALANTARI, A., 1969. Foraminifera from the middle Jurassic-Cretaceous successions of Kopet Dagh region (NE-Iran). Unpublished Ph.D thesis, London University. Exploration and Production Directorate of NIOC, Geological Laboratory Publication 3, Tehran 298 pp.
KALANTARI, A., 1986. Biofacies map of Kopet–Dagh region: NIOC, Exploration and Production, 1 sheet.
KAVOOSI, M.A. and LASEMI, Y., 2005. Sequence stratigraphy of the Cenomanian carbonates of the Sarvak Formation in the Lurestan and Dezful Embayment of the Zagros Basin, southwest Iran. Proceedings of the 9th Annual Meeting of the Geological Society of Iran (in Persian with English abstract).
KAVOOSI, M.A., LASEMI, Y., MOUSSAVI-HARAMI, R. and SHERKATI, S., 2008. Rimmed-shelf transition to carbonate ramp during the Mozduran Formation in Late Kimmeridgian. Proceeding of the 26th annual meeting of the Geological Society of Iran (in Persian with English abstract).
KEUPP, H., JENISCH. A., HERRMANN, R., NEUWEILER, F. and REITNER, J, 1993. Microbial carbonate crusts - a key to the environmental/analysis of fossil spongiolites? *Facies*, **29**, 41-54.
KWON, Y.K., CHOUGH, S.K., CHOI, D.K. and LEE, D.J, 2006. Sequence stratigraphy of the Taebeak Group (Cambrian–Ordovician) Mideast Korea. *Sedimentary Geology*, **192**, 19-55.
LASEMI, Y. 1995. Platform Carbonates of the Upper Jurassic

Mozduran Formation in the Kopet-Dagh Basin, NE Iran–facies paleoenvironments and sequences. *Sedimentary Geology*, **99**, 151–164.

LASEMI, Y. and AMIN-RASOULI, H., 2007. Archaeocyathan build-ups within on entirely siliciclastic succession: New discovery in the Toyonian Lalun Formation of northern Iran, the Proto-Paleotethys passive margin of northern Gondwana. *Sedimentary Geology*, **201**, 302-320.

LASEMI, Y., GHOMASHI, M., AMIN-RASOULI, H. and KHERADMAND,A., 2008.The lower Triassic Sorkh Shale Formation of the Tabas Block, east central Iran: Succession of a failed–rift Basin at the Paleotethys margin. *Carbonates and Evaporites*, **23**, (1), 21-38.

LEEDER, M., 1999. Sedimentology and sedimentary basins. Blackwell Science Ltd, 592pp.

LEINFELDER, R.R., 1993. A modern type Kimmeridgian reef (Ota limestone, Portugal): Implications for Jurassic reef models. *Facies*, **26**, 11-34.

LUCIA, F.J, 1999. Carbonate reservoir characteristics. Springer-Verlag, Heidelberg, 226pp.

LYBERIS, N., and MANBY, G., 1999. Oblique to orthogonal convergence across the Turan block in the Post-Miocene. *AAPG Bull*., **83**, 1135-1160.

MAHBOUBI, A., MOUSSAVI-HARAMI, R., LASEMI, Y., and BRENNER, R.L., 2001. Sequence stratigraphy and sea – level history of the Upper Paleocene strata in the Kopet Dagh Basin, northeastern Iran. *AAPG Bull*., **85**, 839–859.

McILREATH, I.A. and JAMES, N.P., 1984. Carbonate slopes. In: WALKER, R.G., (Ed.): Facies models. *Geoscience Canada*, 245-257.

MONTAÑEZ, I.P. and OSLEGER, D.A., 1993. Parasequence stacking patterns, third-order accommodation events, and sequence stratigraphy of Middle to Upper Cambrian platform carbonates, Bonanza King Formation, Southern Great Basin. In: LOUCKS, R.G. and SARG, J.F., (Eds), Carbonate sequence stratigraphy. *AAPG Mem*., **57**, 305-326.

MOUSSAVI-HARAMI, R. and BRENNER, R.L., 1990. Lower Cretaceous (Neocomian) fluvial deposits in eastern Kopet-Dagh Basin, northeastern Iran. *Cretaceous Research*, **11**, 163-174.

NICHOLS, G., 2000. Sedimentology and stratigraphy. Blackwell Science Ltd, 355pp.

OLIVER, N., HANTZPERGUE, P., GAILLARD, C., PITTET, B., LEINFELDER, R.R., SCHMID, D.U. and WERNER, W., 2003. Microbolite morphology, structure and growth: a model of the Upper Jurassic reefs of the Chay Peninsula (Western France). *Palaeogeography, Palaeoclimatology, Palaeoecology*, **193**, 383-404.

PALMA, R.M., LOPEZ-GOMEZ, J, and PIETHE, R.D., 2007. Oxfordian ramp system (La Manga Formation) in the Bardas Blancas area (Mendoza Province) Neuquen Basin, Argentina: Facies and depositional sequences. *Sedimentary Geology*, **195**, 113-134.

PARCELL, W.C., 2001. Smackover microbial reef detection and characterization. Petroleum Technology Transfer Council, Eastern Gulf Region Symposium.

PAWELLEK, T. and AIGNER, T., 2003. Stratigraphic architecture and gamma ray logs of deeper ramp carbonates (Upper Jurassic, SW Germany). *Sedimentary Geology*, **159**, 203-240.

PETTIJOHN, F.J, POTTER, P.E. and SIEVER, R., 1987. Sand and sandstone. Springer-Verlag, New York, 553pp.

PITTET, B., STRASSER, A. and MATTIOLI, E., 2000. Depositional sequences in deep-shelf environments: A response to sea-level changes and shallow–platform carbonate productivity (Oxfordian, Germany and Spain). *Journal of Sedimentary Research*, **70**, 2, 392-407.

PITTET, B., van BUCHEM, F.P., HILLGARTNER, H., RAZIN, P., GRÖTSCH, T., and DROSTE, H., 2002. Ecological succession, palaeoenvironmental changes, and depositional sequences of Barremian-Aptian shallow-water carbonates in northern Oman. *Sedimentology*, **49**, 555–581.

POURSOLTANI, M.R., MOUSSAVI-HARAMI, R. and GIBLING, M.R., 2007. Jurassic deep–water fans in the Neo-Tethys Ocean, the Kashafrud Formation of the Kopet-Dagh Basin Iran. *Sedimentary Geology*, **198**, 53-74.

PURSER, B.H., 1973. The Persian Gulf Holocene carbonate sedimentation and diagenesis in a shallow epicontinental sea. Heidelberg, Berlin, Springer–Verlag Publication, 471pp.

RASHIDI, M. and TARHANDEH, E., 2007. Hydrocarbon modelling in the Kopet Dagh Basin. Technical report 1506 of National Iranian Oil Company (In Persian), 45 pp.

READ, J.F., 1982. Carbonate platforms of passive continental margins: types, characteristics and evolution. *Tectonophysics*, **81**, 195-212.

READ, J.F., 1985. Carbonate platform facies models. *AAPG Bull*., **66**, 860-878.

RENDEL-BÜHRING, R.H. and REIJMER, J.J.G., 2005. Controls on grain-size patterns in periplatform carbonates: Marginal setting versus glacio-eustacy. *Sedimentary Geology*, **175**, 99-113.

REINECK, H.E. and SINGH, I.B., 1980. Depositional sedimentary environments, with reference to terrigenious clastics, 2nd edition. Springer Verlag, Berlin, 551pp.

RIDING, R., (ED.), 1991. Calcareous algae and stromatolites: New York, Springer Verlag. 577 pp.

RIDING, R., 2006. Microbial carbonate abundance compared with fluctuations in metazoans diversity over geological time. *Sedimentary Geology*, **185**, 229-238.

SCHWARZ, N., SPALLETI, L.A. and HOWELL, J.A., 2006. Sedimentary response to a tectonically induced sea-level fall in a shallow back-arc basin: the Mulichinco Formation (Lower Cretaceous), Neuquen Basin, Argentina. *Sedimentology*, **53**, 55-81.

SEELING, M.T., EMMERICH, A., BECHSTADT, T. and ZUHLKE, R., 2005. Accommodation/sedimentation development and massive early marine cementation: Latemar vs. Concarena (Middle/Upper Triassic, Southern Alps). *Sedimentary Geology*, **175**, 439-457.

SELLEY, R.C., 1996. Ancient sedimentary environments and their sub–surface diagnosis. Chapman and Hall Publication, 300 pp.

SEYED-EMAMI, K., FÜRSICH, F.T., and WILMSEN, M., 2004. Documentation and significance of tectonic events in the northern Tabas block (East–central Iran) during the Middle and Late Jurassic. *Revista Italica di Paleontologia Stratigrafia*, **110**, 1, 163-171.

SHAHRIARI, S., GHAEMI, F., MOUSSAVI-HARAMI, R., and SAEEDI, A., 2005. Tectonic evolution and structural model of Aghdarband tectonic window. *Scientific Quarterly Journal of Geosciences*, **12**, (54), 80-95 (in Persian with English Abstract).

SHINN, E. A., 1983a. Tidal flat environment. In: SCHOLLE, P.A., BEBOUT, D.G. and MOORE, C.H. (Eds), Carbonate depositional environments. *AAPG Mem*oir, **33**, 173-210. AAPG, Tulsa, USA.

SHINN, E.A., 1983b. Birdseyes, fenestrae, shirinkage and loferites: a re-evaluation. *Journal Sedimentary Petrology*, **53**, 619-629.

STRASSSER, A., PITTET, B., HILLGARTNER, H., AND PASQUIER, J.B., 1999. Depositional sequences in shallow carbonate-dominated sedimentary systems: concepts for a high-resolution analysis. *Sedimentary Geology*, **128**, 201-221.

THOMAS, J.C., COBBOLD, P.R., SHEIN, V.S., and Le DOUARAN, S., 1999. Sedimentary record of Late Paleozoic to Recent tectctonism in central Asia–analysis of subsurface data from the Turan and South Kazakh domains. *Tectonophysics*, **313**, 243–263.

TUCKER, M.E. and WRIGHT, V.P., 1990. Carbonate sedimentology. Blackwell Scientific Publication. 482 pp.

ULMISHEK, G., 2004. Petroleum geology and resources of the Amo-Darya Basin, Turkmenistan, Uzbekistan, Afghanistan, and Iran. *USGS Bull*., 2201-4, 32pp.

VAIL, P.R., AUDEMARD, F., BOWMAN, S.A., EISNER, P.N. and PEREZ-CRUZ, C., 1991. The stratigraphic signatures of tectonics, eustasy and sedimentology–an overview. In: EINSELE, G., RICKEN, W. and SEILACHER, A. (Eds): Cycles and events in stratigraphy. Springer Berlin, 617-659.

van BUCHEM, F.S.P., RAZIN, P., HOMEWOOD, P.W., PHILIP, JM., EBERLI, G.P., PLATEL, J-P., ROGER, J, ESCHARD, R., DESAUBLIAUX, G.M.J, BOISSEAU, Th., LEDUC, J-P., LABOURDETTE, R. and CANTALOUBE, S., 1996. High-resolution sequence stratigraphy of the Natih Formation (Cenomanian/Turonian) in northern Oman: Distribution of source rocks and reservoir facies. *GeoArabia*, 1, 1, 65-91.

van WAGONER, JC., POSAMENTIER, H.W., MITCHUM, R.M., VAIL, P.R., SARG, JF., LOUTIT, T.S. and HARDENBOL, J, 1988. An overview of the fundamentals of sequence stratigraphy and key definitions. In: WILGUS, C.K., ROSS, C.A., KENDALL, C.G.St.C., POSAMENTIER, H.W. and VAN, WAGONER, JC., (Eds): Sea-level changes: An integrated approach: *SEPM Special Publication*, 42, 39–45.

van WAGONER, JC., MITCHUM, R.M., CAMPION, K.M. and RAHMANIAN, V.D., 1990. Siliciclastic sequence stratigraphy in Well logs cores, and outcrops. *AAPG Methods in Exploration*, 7, 55 pp.

WHALEN, M.T., EBERLI, G.P., BUCHEM, F.S.P. and MOUNTJOY, E.W., 2000. Facies models and architecture of Upper Devonian carbonate platform (Miette and ancient Wall), Alberta, Canada. In: HOMEWOOD, P.W., and EBERLI, G.P., (Eds): Genetic stratigraphy on the exploration and the production scales. *Elf. Explor. Prod. Mem*., 24, 139–178.

WHALEN, M.T., DAY, J, EBERLI, G.P. and HOMEWOOD, P.T., 2002. Microbial carbonates as indicators of change and biotic crises in carbonate systems: examples from the Late Devonian, Alberta Basin, Canada. *Palaeogeography, Palaeoclimatology, Palaeoecology*, 181, 127-151.

WILSON, JL., 1975. Carbonate facies in geology history. Springer Verlag, New York, 471pp.